CORRIGENDUM

A zebrafish *sox9* gene required for cartilage morphogenesis

Yan, Y.-L., Miller, C. T., Nissen, R., Singer, A., Liu, D., Kirn, A., Draper, B., Willoughby, J., Morcos, P. A., Amsterdam, A., Chung B.-c., Westerfield, M., Haffter, P., Hopkins, N., Kimmel, C. and Postlethwait, J. H. *Development* **129**, 5065-5079.

The name of the third author was published incorrectly in the printed version. The correct name is Robert M. Nissen.

Development 129, 5065-5079 (2002)
Printed in Great Britain © The Company of Biologists Limited 2002
DEV1848

DEVELOPMENT AND DISEASE

A zebrafish *sox9* gene required for cartilage morphogenesis

Yi-Lin Yan[1], Craig T. Miller[1], Robert M. Nissen[2], Amy Singer[1], Dong Liu[1], Anette Kirn[3], Bruce Draper[1,4], John Willoughby[1], Paul A. Morcos[5], Adam Amsterdam[2], Bon-chu Chung[6], Monte Westerfield[1], Pascal Haffter[3], Nancy Hopkins[2], Charles Kimmel[1] and John H. Postlethwait[1,*]

[1]Institute of Neuroscience, University of Oregon, Eugene, OR 97403, USA
[2]Center for Cancer Research, Department of Biology, Massachusetts Institute of Technology, 40 Ames Street, E17-341, Cambridge, MA 02139, USA
[3]MPI für Entwicklungsbiologie, Spemannstr. 35/III, D-72076 Tübingen, Germany
[4]Division of Basic Science, Fred Hutchinson Cancer Research Center, B2-152, 1100 Fairview Ave. N., Seattle, WA 98109-1024, USA
[5]Gene Tools, LLC, One Summerton Way, Philomath, OR 97370, USA
[6]Institute of Molecular Biology, Academia Sinica, Nankang, Taipei, Taiwan ROC
*Author for correspondence (e-mail: jpostle@oregon.uoregon.edu)

Accepted 12 August 2002

SUMMARY

The molecular genetic mechanisms of cartilage construction are incompletely understood. Zebrafish embryos homozygous for *jellyfish* (*jef*) mutations show craniofacial defects and lack cartilage elements of the neurocranium, pharyngeal arches, and pectoral girdle similar to humans with campomelic dysplasia. We show that two alleles of *jef* contain mutations in *sox9a*, one of two zebrafish orthologs of the human transcription factor *SOX9*. A mutation induced by ethyl nitrosourea changed a conserved nucleotide at a splice junction and severely reduced splicing of *sox9a* transcript. A retrovirus insertion into *sox9a* disrupted its DNA-binding domain. Inhibiting splicing of the *sox9a* transcript in wild-type embryos with splice site-directed morpholino antisense oligonucleotides produced a phenotype like *jef* mutant larvae, and caused *sox9a* transcript to accumulate in the nucleus; this accumulation can serve as an assay for the efficacy of a morpholino independent of phenotype. RNase-protection assays showed that in morpholino-injected animals, the percent of splicing inhibition decreased from 80% at 28 hours post fertilization to 45% by 4 days. Homozygous mutant embryos had greatly reduced quantities of *col2a1* message, the major collagen of cartilage. Analysis of *dlx2* expression showed that neural crest specification and migration was normal in *jef* (*sox9a*) embryos. Confocal images of living embryos stained with BODIPY-ceramide revealed at single-cell resolution the formation of precartilage condensations in mutant embryos. Besides the lack of overt cartilage differentiation, pharyngeal arch condensations in *jef* (*sox9a*) mutants lacked three specific morphogenetic behaviors: the stacking of chondrocytes into orderly arrays, the individuation of pharyngeal cartilage organs and the proper shaping of individual cartilages. Despite the severe reduction of cartilages, analysis of *titin* expression showed normal muscle patterning in *jef* (*sox9a*) mutants. Likewise, calcein labeling revealed that early bone formation was largely unaffected in *jef* (*sox9a*) mutants. These studies show that *jef* (*sox9a*) is essential for both morphogenesis of condensations and overt cartilage differentiation.

Key words: *sox9a*, *col2a1*, *titin*, Zebrafish, Chondrogenesis, Pharyngeal arches, Campomelic dysplasia, Cartilage

INTRODUCTION

Cartilage cushions joints and provides a template for the development of cartilage-replacement bones. Aberrant cartilage development results in craniofacial anomalies and cartilage damage results in diseases such as osteoarthritis (Hamerman, 1989). The genetic pathway leading to chondrocyte differentiation is under active investigation (Cancedda et al., 1995; de Crombrugghe et al., 2001), but less is known about the cellular mechanisms that control the assemblage of chondrocytes into higher order cartilage organs. As chondrocytes begin to differentiate, they surround themselves with matrix, including collagen encoded by *COL2A1*. In many cartilages, cells organize themselves into rows called stacks as they begin to form their mature spatial patterns (Kimmel et al., 2001b). Chondrocytes continue directional proliferation, and then hypertrophy. The extracellular matrix mineralizes before the hypertrophic chondrocytes undergo apoptosis and are replaced by their bone-forming cell replacements.

Most cartilage replacement bones fail to develop normally in individuals with campomelic dysplasia (CD), causing

macrocephaly, small jaw, cleft palate, lowset ears and sometimes lack of olfactory bulbs. Individuals with CD often have underdeveloped sclerotome derivatives, including non-mineralized thoracic pedicles and 11, rather than 12, pairs of ribs; and they have poorly developed limbs, including bowed limb bones, hypoplastic scapula and an insufficiently ossified pelvis (Houston et al., 1983; McKusick, 1990; Mansour et al., 1995). In addition, most XY individuals with CD display a variable female phenotype. The cartilage and sex-reversal phenotypes of CD are both caused by mutations in the transcription factor gene *SOX9* (Foster et al., 1994; Wagner et al., 1994; Hageman et al., 1998; Cameron et al., 1996; Huang et al., 1999; Vidal et al., 2001). Individuals with CD are heterozygous for new mutations in *SOX9*, showing that CD is due to a dominant lethal mutation, either from haploinsufficiency or a dominant-negative effect. Mutations in the coding region of *SOX9* or in presumed regulatory elements can cause CD or a similar phenotype in mouse (Wagner et al., 1994; Foster et al., 1994; Kwok et al., 1995; Cameron et al., 1996; Wunderle et al., 1998). Thus, phenotypic analysis of CD shows that *SOX9* is a regulator of chondrogenesis, but because no homozygous tetrapod mutant animals have been observed, and the affected skeletal elements in lethal heterozygotes are merely hypoplastic, we do not know the extent of the function of the gene.

Sox9 belongs to a family of DNA-binding proteins that contain a 79 amino acid long HMG (high mobility group) domain with at least 50% similarity to that of SRY, the sex-determining factor on the Y chromosome (Wright et al., 1993; Wegner, 1999). Sox proteins bind to a seven base pair sequence in the minor groove of DNA (Lefebvre et al., 1997; Ng et al., 1997) and bend DNA (Conner et al., 1994; Werner et al., 1995). Sox9 may also participate in transcript splicing (Ohe et al., 2002). The SOX9 protein has a C-terminal transcription activation domain (Südbeck et al., 1996; Ng et al., 1997), suggesting that it acts by regulating expression of other genes.

Consistent with its role in chondrogenesis, *Sox9* is expressed in the pharyngeal arches and neurocranium, the sclerotomes and the lateral plate mesoderm (Lefebvre et al., 1997; Chiang et al., 2001). In these domains, the expression of *Sox9* slightly precedes and directly regulates the expression of *Col2a1*, which encodes the major collagen of cartilage (Wright et al., 1995; Bell et al., 1997; Lefebvre et al., 1997; Ng et al., 1997; Zhao et al., 1997; Chiang et al., 2001).

Despite this knowledge of Sox9 activity, we have insufficient understanding of the morphogenetic roles Sox9 plays in chondrogenesis or the pathogenesis of CD. Heterozygous *Sox9* mutant mice show phenotypes similar to individuals with CD and die at birth, so permanent lines have not been established (Bi et al., 2001). Delayed or defective pre-cartilaginous condensations are present in heterozygous *Sox9* mutant mouse embryos, but the precise morphogenetic steps that require *Sox9* function remain obscure. Some bones showed premature mineralization in the heterozygous mouse embryos, suggesting that *Sox9* plays a role in regulating the transition to hypertrophic chondrocytes in the growth plates. *Sox9* is thought to regulate this transition by mediating the effects of parathyroid hormone related peptide (PTHrP) (Huang et al., 2001).

We have shown that the zebrafish genome contains two duplicate orthologs of the human *SOX9* gene, called *sox9a* and *sox9b*, and that these map on zebrafish chromosomes that are duplicates of much of human chromosome 17, the location of *SOX9* (Chiang et al., 2001). The two zebrafish *sox9* genes apparently arose in a whole genome duplication event hypothesized to have taken place near the base of the teleost radiation (Postlethwait et al., 1998; Amores et al., 1998). The *sox9a* and *sox9b* genes are expressed in partially overlapping patterns that together approximate the expression pattern of *Sox9* in mouse (Wright et al., 1995; Chiang et al., 2001), as predicted by the duplication, degeneration, complementation hypothesis (Force et al., 1999). Interestingly, however, in zebrafish the testis expresses *sox9a* but the ovary expresses *sox9b* (Chiang et al., 2001), whereas in mammals, only the testis expresses *Sox9* (Morais da Silva et al., 1996). We reasoned that a mutation in one of the two zebrafish genes might not be a dominant lethal mutation as in mammals, and so we investigated recessive lethal zebrafish mutations with phenotypes similar to individuals with CD. We show that two alleles of *jellyfish* (*jef*), one resulting from chemical mutagenesis (*jef*^{tw37}) (Piotrowski et al., 1996; van Eeden et al., 1996) and the other from the insertion of a retrovirus (Amsterdam et al., 1999), disrupt *sox9a*. Confocal microscopy demonstrated that *jef* (*sox9a*) is required not for precartilage condensation formation, but for overt differentiation of cartilage and for three morphogenetic processes: stacking, shaping and individuation. The results suggest that *sox9a* or its downstream targets, perhaps including extracellular matrix proteins, play morphogenetic roles in chondrogenesis.

MATERIALS AND METHODS

Animals, histology and gene expression

The *jef*^{tw37} mutation was identified in an ENU screen for abnormal jaw and fin morphology (Piotrowski et al., 1996; van Eeden et al., 1996). The *hi1134* mutation was isolated in a retroviral insertion screen (Amsterdam et al., 1999). Cartilages were Alcian stained, dissected and flat mounted (Kimmel et al., 1998). Larval bones were visualized with calcein (Molecular Probes, catalog number C-381) (Du et al., 2001) (C. K., unpublished). In situ hybridization was performed as described (Jowett and Yan, 1996) using probes as described (Akimenko et al., 1994; Yan et al., 1995; Chiang et al., 2001). BODIPY-ceramide labeling was performed essentially as described (Cooper et al., 1999). Late epiboly stage embryos were immersed in BODIPY7 FL C5-ceramide (Molecular Probes, catalog number D-3521) dissolved to 10 mM in DMSO, then diluted to 10 μM in Embryo Medium (EM) (Westerfield, 2001) with 10 mM Hepes. Embryos were placed in 150-200 μL of dye solution in 1.2% agarose dishes and stored in the dark. On day 2, embryos were anesthetized, mounted on bridged coverslips, and one side of the head *z*-sectioned at 3 μm intervals with a Zeiss 310 upright confocal microscope. Live developing animals were stored in the dark and at subsequent time points, the same side of each animal was re-examined.

Morpholinos

Morpholino antisense oligonucleotides (MO) were obtained from Gene Tools (Philomath, OR) with the sequences: intron 1 splice donor junction (i1d), AATGAATTACTCACCTCCAAAGTTT; and intron-2 splice donor junction (i2d), CGAGTCAAGTTTAGTGTCCCAC-CTG. Morpholinos were injected as described (Draper et al., 2001). In the i1d MO, the 14th base from the 5′ end, a C, pairs with the G immediately following the splice junction (the one mutated in *jef*^{tw37}). In MO i2d, the 4th base from the 3′ end, a C, pairs with the conserved G just after the splice junction.

Mapping

To map *jef*^{tw37}, we identified a single strand conformation polymorphism (SSCP) (see Postlethwait et al., 1998) in *sox9a* [(mapping primers were sox9a.+9 (CTTTCGCAGACACCAGCAGA) and sox9a –190 (CAGGTAGGGGTCGAGGAGATTCAT)]. Females heterozygous for *jef*^{tw37} were mated to WIK wild-type males, and the F_1 were crossed to make an F_2, which were scored for recombination with microsatellite markers (Knapik et al., 1998; Shimoda et al., 1999) near *sox9a* and *sox9b* (Chiang et al., 2001). The 95% confidence interval around the map distance between *jef*^{tw37} and an SSCP in the 5′ untranslated region of *sox9a* was calculated according to Crow (Crow, 1950). To map the insertion allele *jef*^{hi1134,} we used sox9a-RT2 (CTCCTCCACGAAGGGACGCTTTTCCA), t2a (GGCACTGAGAGTTTTCTGCATCTG) and 5′LTR (AGACCCCACCTGTAGGTTTGGC) (see Fig. 3).

Cloning

Genomic clones of *sox9a* were isolated by amplifying genomic DNA isolated from Oregon AB wild type, Tübingen AB (TÜ, the genetic background of *jef*^{tw37}) or homozygous *jef*^{tw37} embryos. The forward cloning primer binds in the 5′ untranslated region (UTR, sox9a.+11: TTCGCAGACACCAGCAGACAACAAA) and the reverse primer binds near the end of the 3′ UTR (sox9a.-1784: GTCTTTCCCATCATGCACTGAACG). These primers amplified a 3.6 kb fragment including most of exon 1, intron 1, exon 2 and intron 2, and nearly all of exon 3. To minimize PCR errors, Platinum Taq DNA polymerase high fidelity (CAT#11304-029 from Gibco BRL) was used in a touch-down PCR protocol. A BAC-containing *sox9a* (clone 174 (I13)) was identified by screening the BAC zebrafish library-8549 from Incyte Genomics with the primers sox9a.+441 (CCATGCCGGTGAGGGTGAAC) and sox9a.-691 (CTTATAGTCGGGGTGATCTTTCTTGTG). We cloned and sequenced DNA flanking the pro-viral insert linked to the *hi1134* mutant phenotype using inverse PCR as previously described (Amsterdam et al., 1999).

RNA protection assays

Ribonuclease protection assays used the RPA III kit (Ambion, #1414) according to manufacturer's instructions. For each sample, RNA was extracted from about 50 embryos, and 10 μg of total RNA was loaded per lane. The protection probe was a 402 bp long PCR fragment from nucleotide 494 to 896 of the cDNA, including 110 bp of exon 1, all 252 bp of exon 2 and 40 bp of exon-3. The antisense RNA probe for *sox9a* was generated by amplifying a fragment of the *sox9a* cDNA using the primers sox9a.f2 (CCGATGAACGCGTTTATGGTGT) and sox9a.r2 (TTTTCGGGGTGGTGGGAGGAG). The PCR product was cloned into the pCR4-TOP0 vector (Invitrogen; catalog number K4575-J10). The probe was made using MAXIscript Invitro Transcription T3/T7 Kit (catalog number 1326). The amount of protected fragment was quantified using a Storm 860 storage phosphor system (Johnson et al., 1990) with ImageQuant 4.2 software (Molecular Dynamics, Sunnyvale, CA). Normalization used the ubiquitously expressed housekeeping gene *ornithine decarboxylase* (*odc*), expressed sequence tag clone fc54f04; M. Clark and S. Johnson, WUZGR; http//zfish.wustl.edu) as an internal control) (see Draper et al., 2001).

RT-PCR experiments to amplify the *sox9a* message from *jef*^{hi1134} mutants used the primers sox9a.F (CCATGCCGGTGAGGGTGAAC) and sox9a.R (CGTTCGGCGGGAGGTATTGG).

RESULTS

Chondrogenesis requires *jellyfish* activity

Zebrafish homozygous for the recessive lethal ENU-induced *jellyfish* allele *jef*^{tw37} have severely reduced cartilaginous elements (Piotrowski et al., 1996; van Eeden et al., 1996). In wild-type larvae, jaw elements extend anterior and ventral to the eye (Fig. 1A,B), but larvae homozygous for *jef*^{tw37} lack these tissues (Fig. 1E,F) (Piotrowski et al., 1996). Likewise, cartilage supports the fin buds of normal larvae (Fig. 1D), but *jef*^{tw37} larvae have mis-shaped pectoral fins and lack the scapulocoracoid cartilage (Fig. 1F,H) (van Eeden et al., 1996). These phenotypes mimic CD (Houston et al., 1983; McKusick, 1990; Mansour et al., 1995).

A screen for lethal mutations induced by retroviral insertion (Amsterdam et al., 1999; Burgess and Hopkins, 2000) identified a mutation (*hi1134*) giving a phenotype similar to that of *jef*^{tw37} (Fig. 1I-L). To determine whether the *hi1134* mutation is allelic to *jef*^{tw37}, we mated a male heterozygous for *hi1134* to a female heterozygous for *jef*^{tw37} and observed an approx. Mendelian ratio of phenotypically mutant offspring

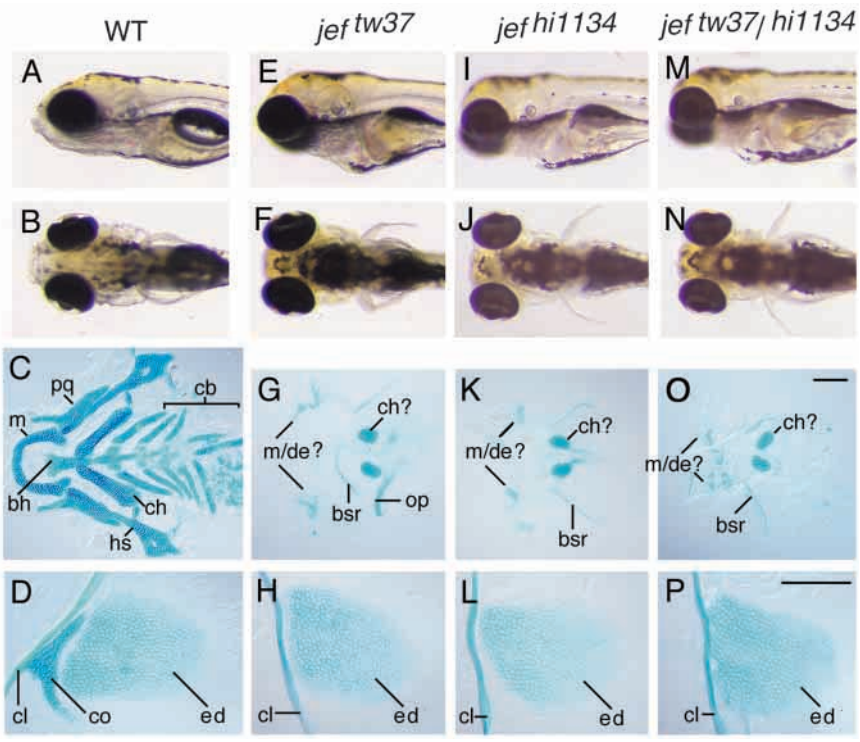

Fig. 1. Activity of *jef* is essential for development of many cartilages. (A,E,I,M, lateral views, anterior towards the left; B,F,J,N, ventral views, anterior towards the left; C,G,K,O, dissected pharyngeal cartilages stained with Alcian, anterior towards the left; D,H,L,P, Alcian stained right pectoral and fin skeletons, anterior towards the top. (A-D) Wild type; (E-H) homozygous *jef*^{tw37}; (I-L) homozygous *jef*^{hi1134}; (M-P) heterozygous *jef*^{tw37}/*jef*^{hi1134}. All animals are 5 dpf. bh, basihyal; bsr, branchiostegal rays; cb, ceratobranchials; ch, ceratohyal; ch?, presumed ceratohyal; cl, cleithrum; ed, endoskeletal disk; co, scapulocoracoid; hs, hyosymplectic; m, Meckel's cartilage; m/de? putative Meckel's cartilage and dentary bone; op, opercule; pq, palatoquadrate. Scale bars: 100 μm in O for C,G,K,O; 100 μm in P for D,H,L,P.

(37 wild-type individuals and nine phenotypically *jellyfish* individuals; Fig. 1M-P). Because these mutations fail to complement, we call the insertion allele *jef*^{hi1134}.

Alcian staining demonstrated that all neurocranial cartilage and most cartilage elements of the pharyngeal arches were missing from animals homozygous for *jef*^{tw37} or *jef*^{hi1134}, or animals heterozygous for the two alleles (Fig. 1C,G,K,O). Small regions of Alcian-positive material remained in both *jef*^{tw37} and *jef*^{hi1134} homozygotes in approximately the position expected for Meckel's cartilage and the ventral region of the ceratohyal cartilage. In addition, cells in the pharyngeal endoderm, possibly mucus secreting cells, were Alcian positive in both wild-type and mutant embryos. In the pectoral girdle, mutant animals lacked the scapulocoracoid cartilage, but the cleithrum bone and endoskeletal disk cartilage appeared normal (Fig. 1D,H,L,P). We conclude that many cartilage elements require *jef* activity.

Molecular genetic nature of *jef*^{tw37}

The *jef*^{tw37} mutation

Because the phenotype of *jef* mutations is similar to the phenotype of people with CD, we tried to rule out that *sox9a* or *sox9b* is disrupted in *jef*^{tw37}. Bulked segregant analysis (Postlethwait et al., 1994) of an F_2 mapping cross revealed linkage to microsatellite marker *z1176* on the upper arm of LG12 near *sox9a*, thus ruling out *sox9b* on LG3 as a candidate. We mapped *jef*^{tw37} at higher resolution relative to a polymorphism in *sox9a*, and uncovered no recombinants between *jef*^{tw37} and *sox9a* among 491 F_2 diploid embryos. This represents 982 meioses, and a distance of 0.1±0.2 cM (centiMorgan) with 95% confidence. Thus, if there are on average 600 kb per cM (Postlethwait et al., 1994), this would be a distance of 60±120 kb. We conclude that *jef*^{tw37} maps very close to or within the *sox9a* gene.

To determine whether *jef*^{tw37} lesions the *sox9a* gene, we cloned and sequenced *sox9a* genomic DNA from homozygous *jef*^{tw37} embryos (Accession Number, AY090036) and compared it with genomic DNA cloned from the wild-type stocks AB (Accession Number, AY090034) and TÜ (Accession Number, AY090035). We found differences between the three strains at 49 locations in the 3560 bp consensus sequence. The two wild-type strains differed at 48 positions, and at the remaining position, the two wild-type strains were the same, but the *jef*^{tw37} strain was different. All but one of the 48 differences between the two wild strains were in non-translated parts of the gene, the exception being a silent change in codon Ala 406. Eleven of the 49 differences were indels between 1 and 10 bp long; the others were single nucleotide differences. The TÜ and *jef*^{tw37} strains differed at only three locations, all of them in introns. In two of those positions, *jef*^{tw37} had the same sequence as the AB wild-type strain, but in the other, the two wild-type strains had a G, but *jef*^{tw37} had a T (Fig. 2A). The unique change was in the first base after the splice donor site of intron 1 in codon Arg146, which alters an *Hph*I restriction endonuclease site, allowing identification of *jef*^{tw37} heterozygotes by PCR.

Because nearly all introns have a G immediately after the splice junction (Mount, 1982; Zhang, 1998), this raised the

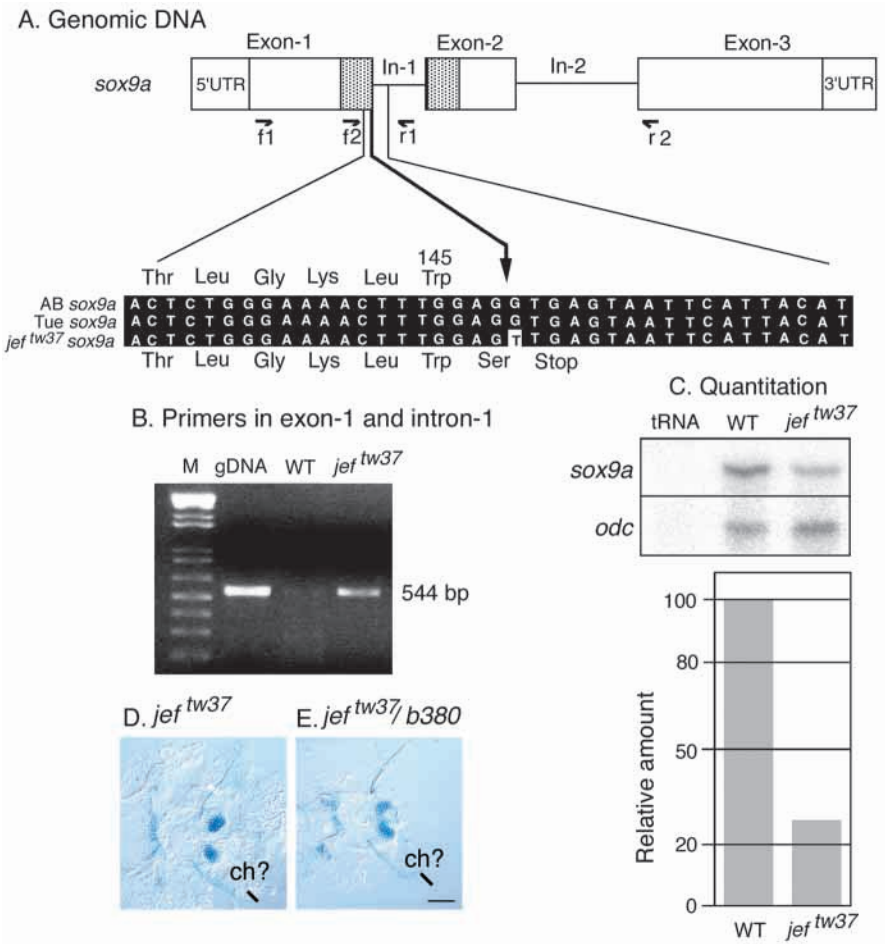

Fig. 2. *jef*^{tw37} alters a conserved splice site sequence in *sox9a* and inhibits message splicing. (A) The sequence of *sox9a* in zebrafish wild-type strains AB and TÜ, splice junction (arrow). An in frame stop codon directly followed the G to T change in *jef*$^{tw37.}$ (B) The primer pair f1/r1 in exon 1 and intron 1 amplified a band of the expected size (544 bp) from wild-type (WT) genomic DNA and from *jef*^{tw37} cDNA, showing that intronic sequences of *sox9a* were present in mutant cDNA. With normal splicing in wild-type cDNA, there was no strong product of this size. (C) RNase protection assays (RPA, upper panel) on RNA extracted from wild-type and homozygous *jef*^{tw37} mutants 4 days old. tRNA served as a negative control. *odc*, the internal control. Probe for RPA is made from a 402 bp of *sox9a* cDNA amplified using primer pair f2/r2. Quantifying band intensity (lower panel) shows a drastic decrease of message in *jef*^{tw37} embryos. (D,E) The *jef*^{tw37} allele behaves as a null when heterozygous for the deletion allele b380. bh, basihyal; bsr, branchiostegal rays; cb, ceratobranchials; ch, ceratohyal; ch?, presumed ceratohyal; cl, cleithrum; ed, endoskeletal disk; co, scapulocoracoid; hs, hyosymplectic; m, Meckel's cartilage; m/de? putative Meckel's cartilage and dentary bone; op, opercule; pq, palatoquadrate. Scale bar: 100 μm.

possibility that the lesion blocks transcript splicing. Because the lesion immediately follows the second nucleotide in codon 146 in the middle of the HMG domain, and an in-frame stop codon follows two codons downstream, a non-spliced transcript should be translated into a truncated protein containing only half of the HMG domain. Such a lesion is likely to lead to an ineffective protein.

The *jef^{tw37}* mutation inhibits splicing

If the G→T transversion in *jef^{tw37}* causes the *jef* phenotype, then it should disrupt the splicing of *sox9a* transcripts. To test this prediction, we made cDNA from homozygous *jef^{tw37}* embryos and their homozygous wild-type siblings, and amplified various regions of the *sox9a* gene (Fig. 2A). A forward primer, f1 in exon 1, and a reverse primer, r1 in intron 1, should fail to amplify a product from mature wild-type *sox9a* mRNA because the mature message lacks intron 1. Unspliced transcripts should give a band of 544 bp. The results showed that genomic DNA from wild-type animals (a positive control) gave a band of the size predicted for a fragment that includes the parts of exon 1 and intron 1, but cDNA from 4-day-old wild-type animals had only a faint band at this location, consistent with normal splicing. By contrast, cDNA extracted from 4-day-old homozygous *jef^{tw37}* animals behaved like wild-type genomic DNA (Fig. 2B), as expected if homozygous *jef^{tw37}* embryos accumulated unspliced transcript.

To learn the extent to which *sox9a* message is reduced in *jef^{tw37}* homozygotes, we prepared cDNA from 4-day-old mutant and wild-type animals, and then conducted RNase protection assays using as probe a region of *sox9a* amplified by primer pair f2 and r2 that includes 110 bp of exon 1, all of exon 2 (251 bp) and 40 bp in exon 3 (Fig. 2A). The ubiquitously expressed housekeeping gene, *ornithine decarboxylase* (*odc*) provided an internal standard (Draper et al., 2001). The results revealed that *jef^{tw37}* embryos possessed only 28% of *sox9a* transcript compared with wild-type animals. We conclude that the mutation drastically decreases the efficiency of *sox9a* transcript splicing.

jef^{tw37} behaves as an amorphic mutation

The molecular genetic analysis of *jef^{tw37}* did not rule out the possibility that some message may be spliced normally in homozygous mutants. Coupled with the remnant bilateral patches of cartilage (Fig. 1G), the protection assays made us concerned that *jef^{tw37}* might be a hypomorph rather than a null allele. The classical test for a null allele is the Müller test: for a null allele, the phenotype of a homozygote equals that of a heterozygote for one mutant allele and one deletion allele (Müller, 1932). To perform this test, we crossed females heterozygous for *jef^{tw37}* to a male heterozygous for the deletion *Df(LG12)dlx3^{b380}* (Fritz et al., 1996), which removes a region of LG12 containing *sox9a* (data not shown). Fifteen of 56 offspring examined showed a *jellyfish* phenotype, and these were confirmed by PCR to be *jef^{tw37}/Df(LG12)dlx3^{b380}*. Fig. 2D,E show that homozygous *jef^{tw37}/jef^{tw37}* animals and heterozygous *jef^{tw37}/Df(LG12)dlx3^{b380}* had the same severity of skeletal phenotype. We conclude that *jef^{tw37}* behaves as a null allele in the Müller test.

Molecular genetic nature of the *jef^{hi1134}* mutation

The *jef^{hi1134}* mutation

An allele with a molecular lesion that deletes protein function would strengthen interpretation of the mutant phenotype. We identified *jef^{hi1134}* in an insertional mutagenesis screen (Amsterdam et al., 1999; Burgess and Hopkins, 2000). The virus inserted into codon Leu147, 2 bp from the 5′ end of exon 2 inside the HMG domain (Fig. 3), which would form a truncated Sox9a protein and probably destroy protein function.

To confirm that the mutant phenotype of *jef^{hi1134}* homozygotes is due to the viral insertion in *sox9a*, we mapped the insertion site with respect to the mutant phenotype. We mated a female heterozygous for *jef^{hi1134}* to the TAB14 wild-type strain and crossed the resulting F_1 progeny to obtain an F_2 mapping population. We scored 66 F_2 individuals for their genotypes by PCR. The mutant and wild-type alleles were distinguished by the forward primer 5′LTR which binds in the insertion, and the forward primer t2a, which binds in intron-1 (Fig. 3). When these are paired with a common reverse primer RT2, which binds in exon-2, the 5′LTR/RT2 primer pair amplified a band of 628 bp with mutant genomic DNA but no band with homozygous wild-type DNA. The t2a/RT2 pair gave a 237 bp fragment with wild-type DNA, and no band with mutant DNA (Fig. 3C). The results showed that of 45 phenotypically mutant F_2 individuals tested, all showed only the 628 bp band expected for homozygous insertions. Of 22 phenotypically wild-type segregants tested, 14 showed both bands expected for heterozygotes and eight showed only the

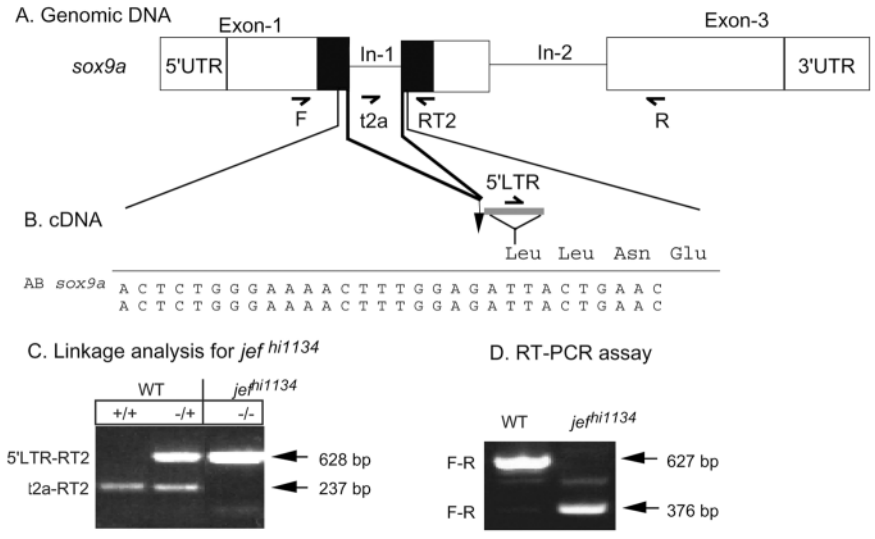

Fig. 3. The *jef^{hi1134}* mutation results from a retroviral insertion into *sox9a* and inhibits the formation of mature message. (A) Primers relative to genomic structure of *sox9a*. (B) A virus inserted into exon 2 in codon Leu147, two base pairs downstream of the intron/exon border in Arg146. 5′LTR indicates the position of a primer. (C) Amplification products of mapping primers (see part A). (D) Primers F and R amplified a band of 627 bp from wild-type (WT) embryos, but a 376 bp band from homozygous *jef^{hi1134}* embryos, showing that exon 2 (251 bp) was skipped in the splicing in *jef^{hi1134}* mutants.

237 bp band expected for wild-type genomic DNA. Thus, among 53 informative individuals, there were no recombinants. This places the insertion within 1.9±11 cM (95% confidence) (Crow, 1950) of the lesion causing the mutant phenotype. Taken with the failure of *jef*^{hi1134} to complement *jef tw37*, we conclude that the viral insertion in *sox9a* is responsible for the *jellyfish* phenotype in *jef*^{hi1134} homozygotes.

The *jef*^{hi1134} mutation inhibits production of mature message

If the insertion in *jef*^{hi1134} causes the mutant phenotype, it could block the formation of mature *sox9a* mRNA by one of at least two mechanisms. First, because it is so close to the splice acceptor site, it might cause the splicing machinery to skip exon 2 entirely. Alternatively, splicing might occur normally, but the message with the insert would be unstable. If the insertion in *jef*^{hi1134} causes skipping of the entire 251 bp exon 2, a primer pair in exon 1 and exon 3 (F/R, Fig. 3) would yield a transcript 251 bp shorter than wild-type. To test these possibilities, we prepared cDNA from mutant and wild-type embryos and amplified the cDNAs. The results showed that in wild type, the predominant band is the 627 bp wild-type product. In mutant animals, however, the predominant band is the 376 bp product produced by neatly skipping exon 2. Direct sequencing of wild-type and mutant PCR products from cDNA confirmed that in *jef*^{hi1134}, exon 1 splices directly to exon 3. Translation of the resulting transcript should add 15 out-of-frame amino acids derived from exon-3 after Leu147. As a final test of *sox9a* expression in mutant embryos, we performed in situ hybridization experiments on wild-type and homozygous *jef*^{hi1134} embryos. The experiments showed reduced signal in the mutant embryos (see Figs 6, 7). Because the viral insertion alters *sox9a* mRNA in a way that would produce a truncated protein with a disrupted HMG box, *jef*^{hi1134} is highly likely to be a null mutation.

Inhibition of *sox9a* function with morpholinos

Morpholinos against *sox9a* produce a phenotype similar to *jef*

To confirm that reduction in *sox9a* function results in the *jef* phenotype, we injected embryos with morpholino antisense oligonucleotides targeted to *sox9a*. Injecting homozygous wild-type embryos with 5.0 mg/ml of two splice junction MOs (i1d and i2d) greatly reduced cartilage in the pharyngeal arches (Fig. 4E). Treating the offspring of heterozygous *jef*^{tw37} males and females with sox9a MOs gave animals in three phenotypic classes. Some animals had hypoplastic but recognizable cartilages (Fig. 4E); others had rudimentary first and second arch cartilage elements with two rather large blocks of cartilage remaining at about the location of the ceratohyal (Fig. 4H); and some animals had the typical homozygous *jef*^{tw37} phenotype, with two small blocks of Alcian-positive material remaining (Fig. 4K). Genotyping the animals for the *Hph*I site polymorphism in *jef*^{tw37} before Alcian staining showed that among 91 animals, the least severely affected class (20 animals, 22%) were all homozygous wild type; the intermediate class (47 animals, 51%) were all heterozygotes; and the animals with the severe phenotype were all homozygous *jef*^{tw37} (24 animals, 26%). These genotypes were found in the ratio of ~1:2:1 as expected in the progeny of two heterozygotes. We conclude that heterozygous *jef* animals are more sensitive to sox9a MO than homozygous wild-type animals. The series of phenotypes found in these experiments suggests that the remnant bilateral Alcian-positive regions in *jef* animals may be portions of the ceratohyal.

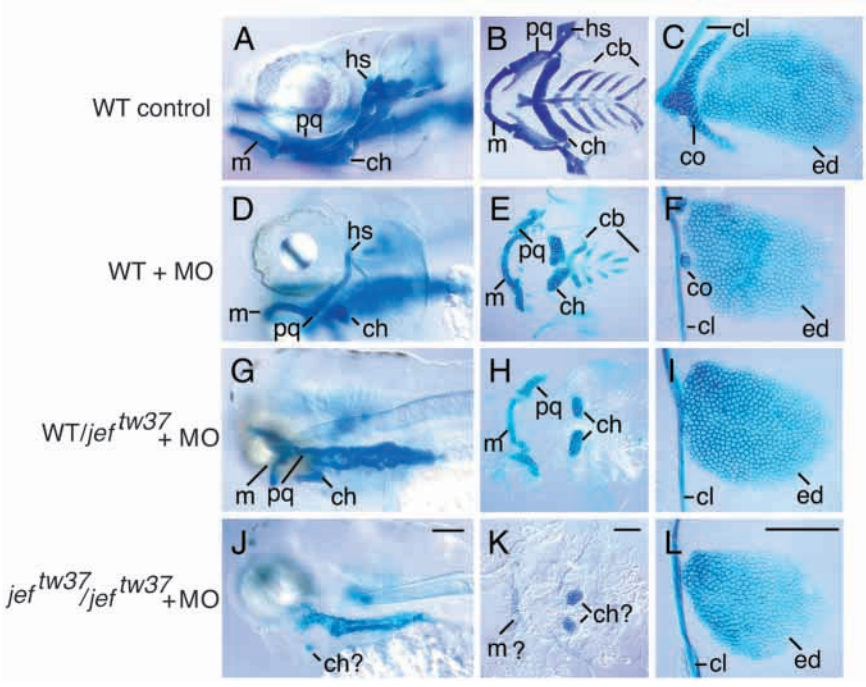

Fig. 4. Splice-directed morpholinos to *sox9a* produce a phenotype similar to *jef*. (A-C) Uninjected wild-type controls. (D-F) Homozygous wild types injected with MO i1d plus i2d. (G-I) Heterozygotes for *jef*^{tw37} injected with MOs. (J-L) MO injected homozygous *jef*^{tw37} individuals. (A,D,G,J) Lateral view of 5 dpf animals, anterior towards the left. (B,E,H,K) Ventral view of dissected cartilages, anterior towards the left. (C,F,I,L) Right pectoral and fin skeleton, proximal towards the left. bh, basihyal; bsr, branchiostegal rays; cb, ceratobranchials; ch, ceratohyal; ch?, presumed ceratohyal; cl, cleithrum; ed, endoskeletal disk; co, scapulocoracoid; hs, hyosymplectic; m, Meckel's cartilage; m/de? putative Meckel's cartilage and dentary bone; op, opercule; pq, palatoquadrate. Scale bars: in J, 100 μm for A,D,G,J; in K, 100 μm for B,E,H,K; in L, 100 μm for C,F,I,L.

The pectoral fin skeletons of MO-injected animals showed a similar pattern. Alcian stained wild-type pectoral fins at 5 dpf (days post-fertilization) showed a flat endoskeletal disc, the basal scapulocoracoid of the pectoral girdle, and the cleithrum, a long straight bone (Fig. 4C) (see Grandel and Schulte-Merker, 1998). The scapulocoracoid cartilage was missing in homozygous and heterozygous *jef*^{tw37} animals treated with MO, but the endoskeletal disk and cleithrum were nearly normal (Fig. 4I,L). The scapulocoracoid in the pectoral fins of homozygous wild-type animals injected with the MOs was reduced to two small patches of six to ten cells (Fig. 4F).

To determine the efficacy of splice-

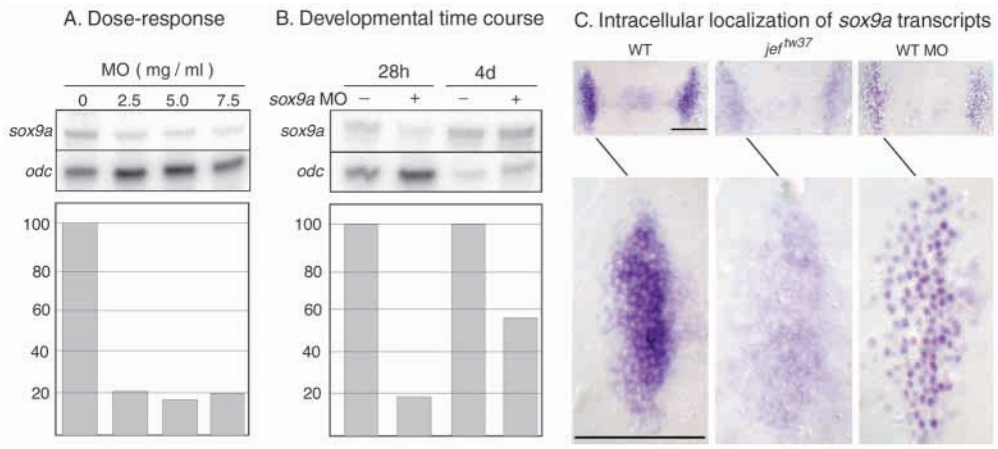

Fig. 5. Morpholino antisense oligonucleotides directed against *sox9a* inhibit splicing and transport of *sox9a* transcript. (A) RNase protection assays of *sox9a* transcript in 28 hpf wild-type animals injected at the one-cell stage with 2 nl of different concentrations of MO, normalized against *odc*. (B) RNase protection assays of *sox9a* transcript in animals 28 hpf or 4 dpf either treated (+) or not treated (–) with 5.0 ng MO, normalized against *odc*. Graphs show the amount of RNA present as a percent of untreated controls. (C) Transcript for *sox9a* accumulates in the cytoplasm in wild type, but in the nucleus in splice-directed MO injected embryos at 28 hpf. In *jef*^{tw37} embryos, transcript is visible both in the cytoplasm and in the nucleus. Dorsal views, anterior is upwards. Equal amounts of MO directed against the donor sites for intron 1 and 2. Scale bars: 100 μm.

directed MOs to inhibit transcript splicing, we injected one-cell embryos with MO i1d and i2d. Solutions contained equal quantities of both MOs at final total concentrations of 2.5, 5.0 and 7.5 mg/ml, and we injected about 2 nl into each embryo. We quantified the results in RNase protection assays conducted on RNAs collected from either 28 hpf (hours post-fertilization) embryos or 4-day-old larvae. The *odc* gene served as an internal control. The results showed that embryos injected with even the lowest dose tested showed levels of spliced *sox9a* transcript only about 20% of normal at 28 hpf (Fig. 5A). To determine how long in development the morpholino would have an effect, we compared the inhibition of splicing in 28 hpf embryos to that in 4 dpf animals for the intermediate dose of MO. The results showed that by 4 dpf, the amount of normal-sized transcript had increased to about 55% of that found in untreated controls (Fig. 5B). We conclude that these MOs provide a significant inhibition of transcript splicing in the first day of embryonic life, but by day 4, the effects of the MOs on transcript splicing had begun to wane, presumably due to dilution of the MOs associated with cell proliferation.

Inhibiting splicing with morpholinos alters the intracellular distribution of *sox9a* transcript

In normal wild-type animals, *sox9a* transcript accumulates in the cytoplasm (Fig. 5C). Does the mutation in the splice-donor site or a splice-inhibiting MO hinder the transport of transcript to the cytoplasm? By the two-somite stage (Fig. 5C), the cytoplasm of presumptive cranial placode cells accumulated substantial quantities of *sox9a* transcript in wild-type embryos. By contrast, the difference in transcript amount between the cytoplasm and the nucleus of the corresponding cells in *jef*^{tw37} embryos is rather small (Fig. 5C). Wild-type animals treated with the splice junction MOs i1d and i2d showed no apparent *sox9a* transcript in the cytoplasm, but accumulated substantial quantities of transcript in the nucleus. We conclude that MOs directed against a splice junction can block the transport of transcript from the nucleus to the cytoplasm. The inappropriate localization of transcript can provide an assay for MO efficacy in the absence of an antibody to test for the production of a translated product.

The MO results allow several conclusions. First, the similarity of *sox9a* MO and *jellyfish* phenotypes supports the conclusion that *jef* mutations disrupt the function of *sox9a*; we therefore call this gene *jef* (*sox9a*) according to zebrafish nomenclature guidelines (http://zfin.org/zf_info/nomen.html). Second, the failure of the splice-junction MOs to enhance the phenotype of *jef*^{tw37} homozygotes is consistent with the interpretation of *jef*^{tw37} as a null allele. Third, the results suggest that both mutant alleles of *jef* are more effective at knocking down *sox9a* activity than are the MOs, perhaps because the morpholinos are less effective at blocking a late phenotype. And fourth, the accumulation of transcript in the nucleus with splice-directed morpholinos can provide an assay for morpholino efficacy independent of phenotype.

An essential role for *sox9a* in chondrogenesis

These results show that *jef* (*sox9a*) is essential for the formation of cartilages in the neurocranium, pharyngeal arches and pectoral appendages, but do not reveal which step in cartilage formation requires the gene. If *jef* (*sox9a*) is required for the migration of crest cells, cranial crest, as marked by *dlx2* expression (Akimenko et al., 1994), should be aberrant in homozygous *jef*^{tw37} embryos. In situ hybridization experiments showed that *dlx2* and *sox9a* are expressed in the same groups of cells in 30-somite stage wild-type embryos (Fig. 6 and data not shown). In homozygous *jef*^{tw37} and *jef*^{hi1134} embryos, *sox9a* transcript is weakly detected at this stage (Fig. 6C,E), but the expression pattern of *dlx2* is unperturbed (Fig. 6D,F). These results suggest that *sox9a* is not required for the specification of cranial crest or for the migration of crest cells into the pharyngeal arches.

To determine if postmigratory cranial neural crest is properly specified in *jef* mutants, we examined two markers of ventral postmigratory crest, *dhand* and *epha3* (Miller et al., 2000). Expression of these genes at 36 hpf showed no distinguishable alterations in *jef* mutants (data not shown). Thus, at least the ventral postmigratory pharyngeal arch crest in *jef* mutants is properly specified with respect to these two markers.

The expression of *col2a1* marks differentiating chondrocytes in zebrafish (Yan et al., 1995) and *Col2a1* is essential for proper chondrogenesis in mammals (Vandenberg et al., 1991). To determine whether *jef* (*sox9a*) is essential for *col2a1* expression in pharyngeal arches, we compared the expression domains of *sox9a* and *col2a1* in wild-type embryos, and tested whether the expression of *col2a1* was altered in *jef* (*sox9a*) homozygotes.

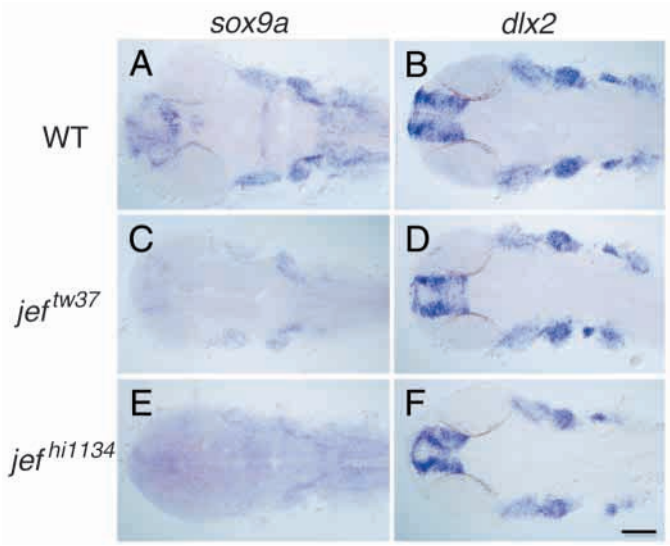

Fig. 6. Activity of *sox9a* is not required for the specification or migration of cranial neural crest. (A,B) Wild type (WT) embryos. (C,D) Homozygous *jef*^{tw37} embryos. (E,F) Homozygous *jef*^{hi1134} embryos. (A,C,E) *sox9a* expression. (B,D,F) *dlx2* expression. All animals were 24 hpf. Dorsal views, anterior towards the left.

The results show that the neurocranium, pharyngeal arches and pectoral fins co-express *col2a1* and *sox9a* in wild-type embryos (Fig. 7A,B,G,H), although *col2a1* shows additional expression in the presumptive precursors of the cartilage capsule of the ear and eye. In mutant animals, *sox9a* expression is reduced (Fig. 7C-F), and *col2a1* expression appears in only small regions of the pharyngeal arches (Fig. 7I-L). Ventral groups of cells in the first and second arches retain *col2a1* expression. The expression in the second arch may correspond to the remaining bilateral Alcian-positive patches found later in mutant animals (see Fig. 1C,G,K,O). These results show that in much of the pharyngeal arch skeleton, the expression of *col2a1* depends on *sox9a* activity.

Prechondrogenic condensations form in *jef* (*sox9a*) mutants, but cartilage differentiation and condensation morphogenesis fail to occur

Because migratory and postmigratory cranial neural crest are present in *jef* (*sox9a*) mutant embryos (Fig. 6), the severe reduction of differentiated (Alcian-positive) cranial cartilage seen later in *jef* (*sox9a*) mutant larvae is due either to the failure of prechondrogenic condensation formation or to the failure of condensation progression into differentiated cartilage. To distinguish between these possibilities, we mated heterozygous *jef* (*sox9a*) males and females, and labeled the resulting embryos with the vital fluorescent dye BODIPY-ceramide. This dye fills extracellular spaces, thus labeling cell outlines, and has the powerful advantage of allowing histological identification of nearly every cell type in live preparations (Cooper and Kimmel, 1998). We examined live developing BODIPY-ceramide-stained larvae at multiple time points from 48 hours, when no pharyngeal cartilage differentiation had occurred in wild types (Schilling and Kimmel, 1997), until 76 hours, when the primary scaffold of the larval pharyngeal skeleton had chondrified. At 48 hours, wild type and mutants for both mutant alleles of *jef* (*sox9a*) had precartilage condensations in the first two pharyngeal arches (Fig. 8A-B′ and data not shown). Although at this stage no differentiated (Alcian-positive) pharyngeal cartilage was present (Schilling and Kimmel, 1997), the primordia of the major cartilages in the first two arches were readily identifiable in wild type and mutant (Fig. 8A-B′). For example, the hyomandibular foramen was present, as was the rudiment of the symplectic (Fig. 8A-B′). By 54 hours, differentiation had begun in wild type (Schilling and Kimmel, 1997), but had failed to occur in *jef* (*sox9a*) mutants (data not shown). Concomitant with differentiation, in wild-type embryos chondrocytes organized into orderly stacks (data not shown) (Kimmel et al., 1998).

By 76 hours, cartilages in the first and second arches of wild-type embryos were well-formed, whereas *jef* (*sox9a*) mutants had failed to undergo three major morphogenetic processes. First, *jef* (*sox9a*) mutants failed to form stacks of chondrocytes (Fig. 8C-D′ and data not shown), but cells in wild-type precartilage condensations oriented themselves with their long axes parallel to each other (Fig. 8C,C′) (Kimmel et al., 1998). The only pharyngeal cartilages to differentiate in *jef* (*sox9a*) mutants, the small bilateral nodules of disorderly cartilage that form in the ventral second arch (see Figs 1, 4) lacked orderly stacks of chondrocytes. Second, the precartilage condensations in *jef* (*sox9a*) mutants failed to separate into individualized regions. For example, the prominent dorsal/ventral joint that

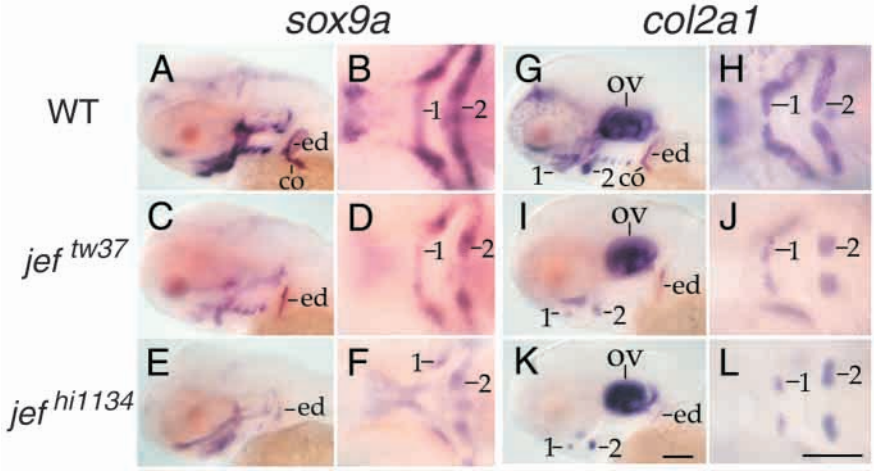

Fig. 7. Activity of *sox9a* is necessary for the expression of *col2a1* in most developing cartilage of the neurocranial, pharyngeal and pectoral skeleton. (A-F) Expression of *sox9a*. (G-L) Expression of *col2a1*. (A,B,G,H) Wild-type animals. (C,D,I,J) Homozygous mutant *jef*^{tw37} embryos. (E,F,K,L) Homozygous mutant *jef*^{hi1134} embryos. Photographs are a montage with focus on the pharyngeal cartilages, and the pectoral girdle. All animals are 68 hpf. 1 and 2, first and second pharyngeal arches; co, scapulocoracoid; ed, endoskeletal disc; ov, otic vesicle. (A,C,E,G,I,K) Lateral views, anterior towards the left. (B,D,F,H,J,L) Ventral views, anterior towards the left. Scale bars: in K, 100 μm for A,C,E,G,I,K; in L, 100 μm for B,D,F,H,J,L.

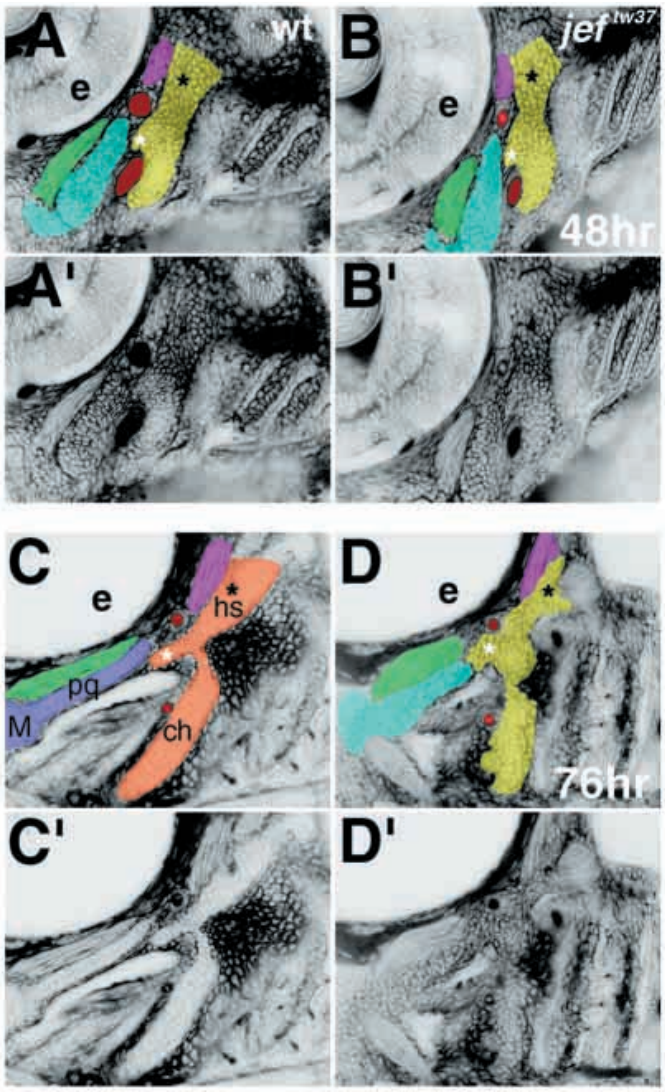

Fig. 8. Prechondrogenic condensations form in *jef* (*sox9a*) mutants, but differentiation and morphogenesis fail to occur. Confocal micrographs (lateral views shown as negative images, anterior towards the left) of live wild-type (A,A′,C,C′) and *jef*^{tw37} mutants (B,B′,D,D′), stained with BODIPY-ceramide. Cells appear white and interstitial space appears black. (The pharyngeal cavity does not retain the dye, so it also appears white in C-D′). At 48 hours, in wild types (A,A′) and *jef* mutants for both alleles (B,B′, and data not shown), prechondrogenic condensations have formed. The original images (A′,B′) are pseudo-colored (A,B) to highlight the first (blue) and second (yellow) pharyngeal arch precartilage condensations. Red, first aortic arch; green, adductor mandibulae muscle; pink, constrictor dorsalis premyogenic condensation. At this stage, a contiguous condensation prefigures the dorsal and ventral pharyngeal cartilages, as seen best for the second arch in this focal plane (A-B′). In the second arch precartilage condensation, the symplectic rudiment (white asterisk) and hyomandibular foramen (black asterisk) are apparent in wild types and *jef* mutants (A-B′). By 76 hours, individuated and precisely shaped dorsal and ventral first and second pharyngeal arch cartilages with highly ordered stacks of chondrocytes have formed in wild types (C,C′). Original images (C′,D′) are pseudocolored (C,D as in A,B) with overtly differentiated cartilage in wild types colored purple in the first arch and orange in the second arch cartilages. Stacking, individuation, and proper shaping do not occur in *jef* mutants (D,D′). The precise boundary of the first and second arch is not visible in *jef* mutants and is approximated in the pseudocolored panel (D). For *jef*^{tw37}, five mutants and 15 phenotypically wild-type siblings were examined; for *jef*^{hi1134}, nine mutants and 21 phenotypically wild-type siblings were examined. ch, ceratohyal; e, eye; hs, hyosymplectic; M, Meckel's; pq, palatoquadrate (see Fig. 1).

separates the upper and lower jaw (palatoquadrate and Meckel's, Fig. 8C-D′) in wild-type embryos was undetectable in *jef* (*sox9a*) mutants. Third, *jef* (*sox9a*) mutant precartilage condensations failed to transform into the specific shapes of their wild-type counterparts. For example, the symplectic region of wild-type embryos formed a long, orderly rod of cartilage, whereas this region in *jef* (*sox9a*) mutants was deformed into a jumbled region of mesenchyme (Fig. 8C-D′). For both mutant *jef* (*sox9a*) alleles, the phenotypically wild-type siblings (which should have included both heterozygotes and wild-type homozygotes) were indistinguishable from one another. Thus, at this single-cell level of analysis, no evidence for heterozygous phenotype in either allele was seen, consistent with the lack of a detectable heterozygous phenotype by Alcian staining.

These data show that *jef* (*sox9a*) function is not required for formation of pharyngeal precartilage condensations, but rather for subsequent differentiation of cells within the condensations. Furthermore, *jef* (*sox9a*) function is required for three morphogenetic processes: formation of orderly stacks, the individualization of cartilages and the shaping of specific skeletal elements.

Chondrogenesis and muscle patterning

Signals from the cranial neural crest are required to pattern the mesodermally derived muscles of the pharynx (Noden, 1983; Schilling et al., 1996). Cranial neural crest gives rise to muscle connective tissue (Kontges and Lumsden, 1996), which could be one source of this signal. Alternatively, cartilage precursors or the cartilages themselves might signal muscle patterning. Given the widespread expression of *sox9a* in cranial crest and the severe defect in cartilage differentiation in *jef* (*sox9a*) mutants, *jef* mutants might have defects in muscle patterning from one of these sources. To test this possibility, we cloned and mapped a fragment of the muscle gene *titin* (GenBank Accession Number AY081167) (Xu et al., 2002) to use as a marker for muscle cells. A single molecule of Titin (the largest protein known) spans half the length of a sarcomere (Labeit and Kolmerer, 1995). We report here the mapping of the zebrafish *ttn* gene to LG9 at 109.8 cM on the heat shock panel (Woods et al., 2000), a region of conserved synteny with the long arm of human chromosome 2, the site of the human *TTN* gene. Expression of *ttn* showed a full complement of pharyngeal muscles in *jef* animals homozygous for either allele (Fig. 9). Although the positions and shapes of muscles were slightly distorted, presumably because of the absence of cartilage-derived skeletal elements for muscle insertions, the pattern-forming process was normal in *jef* mutants. We conclude that *jef* (*sox9a*) activity is not required to pattern these anterior pharyngeal muscles.

Early bone formation is largely unaffected in *jef(sox9a)* mutants

Mice heterozygous for a *Sox9* mutation exhibit expanded

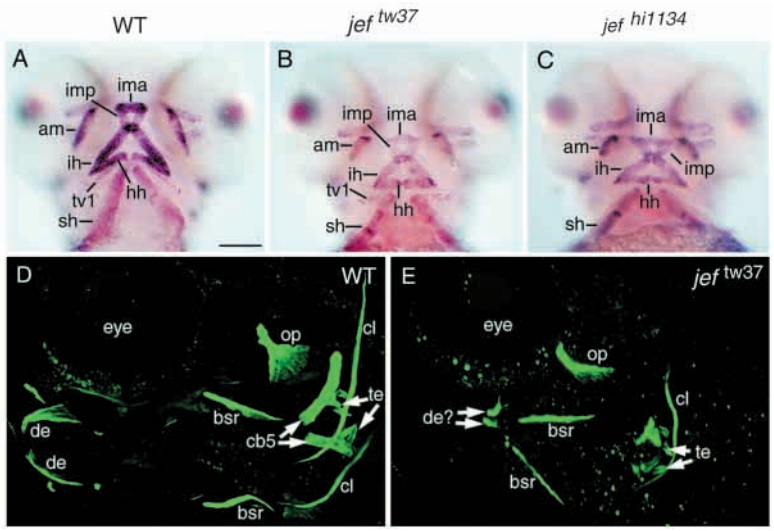

Fig. 9. Muscle and bone in *jef* mutants. Expression of *titin* in wild-type (A) and homozygous *jef*^{tw37} (B) and *jef*^{hi1134} (C) animals at 3 dpf reveals normal patterning of cranial muscles. Compiled stacks of confocal micrographs of wild-type (D) and a *jef*^{tw37} mutant (E) stained with calcein. Most dermal bones (op, bsr, cl) are relatively unaffected in *jef* mutants, whereas the dermal dentary (de) and cartilage replacement fifth ceratobranchial bone (cb5) are severely reduced. Teeth (te) are present, as are tiny remnants of bone at the base of the teeth. Bone development occurs on schedule without enlarged ossification centers in *jef* mutants. am, adductor mandibulae; bsr, branchiostegal ray; cb5, fifth ceratobranchial; cl, cleithrum; de, dentary; hh, hyohyoideus; ih, interhyoideus; ima, intermandibularis anterior; imp, intermandibularis posterior; op, opercle; sh, sternohyoideus; te, teeth; tv1, transversus ventralis. Scale bar: in A, 100 μm for A-C.

ossification centers that prematurely ossify (Bi et al., 2001). To learn whether *jef* (*sox9a*) mutants show these phenotypes, we examined larval bone development in *jef* (*sox9a*) mutant larvae using the fluorescent dye calcein (Du et al., 2001) (C. K., unpublished). Despite the severe cartilage defects in *jef* (*sox9a*) mutants, most major cranial and pectoral fin bones appeared on schedule and were only slightly reduced in size in *jef* (*sox9a*) mutants (Fig. 9E, and data not shown). The second arch dermal opercles and branchiostegal rays appeared on schedule in *jef* (*sox9a*) mutants and were mildly reduced. The blade of the *jef* (*sox9a*) mutant opercular bone was reduced ventrally and displaced anteriorly towards the eye. The cleithrum in the fin girdle was present (Fig. 9, see also Fig. 1D,H,L,P), as were pharyngeal teeth (Fig. 9). By contrast, the fifth ceratobranchial bone, which is a cartilage replacement bone (Cubbage and Mabee, 1996), was strikingly absent in *jef* (*sox9a*) mutants. Tiny remnants of bone were present adjacent to the teeth of *jef* (*sox9a*) mutants, perhaps the bone of attachment of the teeth or the severely reduced remnant of the fifth ceratobranchial bone. Small remnants of bone were also present in *jef* (*sox9a*) mutants in the position of the wild-type dentary, which normally forms in the lower jaw. Examining *jef* (*sox9a*) mutants at earlier time points (days 3 and 4) revealed no evidence for precocious bone development or enlarged ossification centers (data not shown). The early larval lethality of *jef* mutants thwarts analysis of ribs and other later-forming skeletal structures, as well as frustrating the analysis of gonad morphogenesis.

DISCUSSION

These experiments identify *jef* as a mutation in *sox9a*, one of the two zebrafish orthologs of the human *SOX9* gene. Evidence for this conclusion comes from the sequencing of *sox9a* from animals homozygous for either of two *jef* alleles, one induced by ENU and the other by retroviral insertion. The ENU-induced mutation changed a conserved G immediately following the splice junction (Mount, 1982; Kreivi and Lamond, 1996). Mutations of this nucleotide at the corresponding site in the second intron of the human *SOX9* gene can cause CD (Wagner et al., 1994), and similar mutations disrupt many other genes in humans (Freddi et al., 2000; Sironi et al., 2001; Targovnik et al., 2001) and in zebrafish (Lun and Brand, 1998; Childs et al., 2000). A quantitative assay for *sox9a* transcript and in situ experiments confirmed that the mutation in *jef*^{tw37} severely inhibits splicing of the *sox9a* transcript. The insertion allele results in the skipping of exon 2, and the predicted subsequent translation of a short protein truncated within exon 3.

Two *jef* (*sox9a*) alleles behave as null mutations

To infer the role of a gene from its mutant phenotype, it is essential to know whether the alleles investigated lack all function of the gene. This is relevant here because, first, the mammalian mutants retain one normal *SOX9* allele and, second. because the zebrafish mutants retain a small patch of Alcian-positive material in the location of the second arch. The zebrafish phenotype could result either from residual activity of *sox9a* from the mutant allele, or from activity of a different gene. We conclude that the two *jef* (*sox9a*) alleles are likely null alleles because: (1) the viral insertion in *jef*^{hi1134} causes the skipping of exon 2, which should result in a truncated protein; (2) animals heterozygous for *jef*^{tw37} over a deletion do not have a more severe phenotype than *jef*^{tw37} homozygotes; (3) morpholinos that affect wild-type and heterozygous embryos do not make the *jef*^{tw37} phenotype more severe; and (4) the phenotype of *jef*^{tw37}/*jef*^{hi1134} heterozygotes have the same phenotype as either homozygote.

Splice-directed morpholinos provide an independent assay for efficacy

Animals injected with splice-directed morpholinos displayed a weaker phenotype at day 4 than did homozygous *jef*(*sox9a*) mutations, presumably because of to the rebound of transcript splicing as evidenced by the RNase protection assays. MO-treated animals accumulated *sox9a* transcript in the nuclei of *sox9a*-expressing cells, apparently because of a defect in transcript transport. We have also observed this phenomenon for splice-directed morpholinos against *sox9b* (Y.-L. Y., unpublished). Although it is well known that MOs can inhibit splicing (Schmajuk et al., 1999; Draper et al., 2001), to our

knowledge this inhibition had not previously been shown to retard the transport of transcript to the cytoplasm. Our novel finding provides an assay for MO efficacy independent of any phenotypic change. This assay or the RNase protection assay, is generally more convenient than an assay for the efficacy of a translation-inhibiting MO because probes to measure nucleic acid quantity are much more readily available than probes to measure the quantity of a specific protein, which often requires a specific antibody. Furthermore, as pointed out by Draper et al. (Draper et al., 2001), splice-directed morpholinos may allow one to distinguish between the effects of different splice variants, and to distinguish between the functions of maternal and zygotic transcript.

Evaluating *jef* (*sox9a*) mutants as a model for campomelic dysplasia

People affected with CD are heterozygous for a mutation in *SOX9*, and display a syndrome of clinical features that include bowing of the tibia and femur, hypoplastic scapula, absence of a pair of ribs, cleft palate and a small jaw (Houston et al., 1983; McKusick, 1990; Foster et al., 1994; Wagner et al., 1994; Kwok et al., 1995; Mansour et al., 1995; Cameron et al., 1996; Hageman et al., 1998). Zebrafish homozygous for *jef* (*sox9a*) mutations mimic at least two of these phenotypes, but show them in more severe form. In humans and mice (Bi et al., 1999; Bi et al., 2001) heterozygous for *SOX9* mutations, the scapulas and jaws form, but they are small and thin. By contrast, the corresponding elements in zebrafish *jef* (*sox9a*) mutants, the scapulocoracoid cartilage and the first and second arch derivatives, are almost completely gone.

Why is the zebrafish *sox9a* mutant phenotype more severe in these aspects than the mammalian *SOX9* mutant phenotypes? This question is significant because we need to know whether *SOX9* is essential for development of these elements or whether it merely facilitates completion of these cartilages. Many *SOX9* mutations in mammals are likely to be null activity alleles rather than dominant negative mutations, judging from their predicted effect on the proteins (Foster et al., 1994; Wagner et al., 1994; Kwok et al., 1995; Mansour et al., 1995; Cameron et al., 1996; Hageman et al., 1998; Bi et al., 1999; Bi et al., 2001). Thus, the heterozygotes probably have about half the normal amount of *SOX9* activity in tissues in which the gene is expressed. Homozygous *jef* (*sox9a*) animals should completely lack *sox9* activity in all cells in which *sox9a* is expressed in the absence of *sox9b*. Before hatching, the time during which the *jef* (*sox9a*) phenotype becomes apparent, *sox9a* is expressed strongly in the first and second arches and in the scapulocoracoid, but *sox9b* is not expressed in these cells (Chiang et al., 2001). We therefore conclude that *SOX9* activity is essential for chondrogenesis of the arches, neurocranium and scapulocoracoid, and that mammals show a weak phenotype because *SOX9* activity is reduced, but not completely lost, in the mammalian heterozygous genotypes. The evolution of duplicated zebrafish genes has thus allowed analysis of null-activity embryos not yet available for the ortholog in mammals.

Many individuals with CD have XY sex reversal (Houston et al., 1983; McKusick, 1990; Foster et al., 1994; Wagner et al., 1994; Kwok et al., 1995; Mansour et al., 1995; Cameron et al., 1996; Hageman et al., 1998). Although *sox9a* is expressed in the zebrafish testis, and *sox9b* is expressed in the zebrafish ovary (Chiang et al., 2001), consistent with a role in sex determination, the late determination of sex in zebrafish has so far precluded the investigation of sex determination in *jef* (*sox9a*) animals. Because both male and female animals heterozygous for *jef* (*sox9a*) become sexually mature adults of both sexes, *jef* (*sox9a*) appears not to have a fully penetrant dominant effect on sex determination in zebrafish.

Prechondrogenic condensations form in *jef* (*sox9a*) mutants

The formation of prechondrogenic condensations in *jef* (*sox9a*) mutant zebrafish suggests that *sox9a* is not required for condensation formation in zebrafish. The opposite conclusion was drawn for mouse. Because cells homozygous for a *Sox9* mutation failed to contribute to condensations in genetic mosaics, Bi et al. (Bi et al., 1999) concluded that *Sox9* was required for formation of condensations. These differences might reflect: (1) species differences in *SOX9* function; (2) the presence of duplicated s*ox9* genes in zebrafish; and/or (3) the difference in experimental paradigms used. Although *jef* (*sox9a*) mutant cells form condensations in the context of a totally mutant environment, they might not contribute to condensations when transplanted into a wild-type host, as was found with mouse. Mosaic analyses in zebrafish could test this possibility.

Support for the idea that differences in experimental paradigms could explain the contrasting conclusions on the requirement of *SOX9* for condensation formation comes from analysis of the zebrafish *valentino* mutant. Embryos that lack *val* (*mafb*) activity make hindbrain tissue between rhombomeres 4 and 7, yet in genetic mosaics, *val* (*mafb*) mutant cells are excluded from this territory in a wild-type host (Moens et al., 1996). Thus, by analogy, homozygous *Sox9* mutant mice, like *sox9a* mutant zebrafish, might form precartilage condensations even though mutant cells are excluded from these domains in a mosaic. A mammalian phenotype analogous to that seen in zebrafish *jef* (*sox9a*) mutants might be the *L-Sox5; Sox6* double mutant in mouse, where condensations form, but no overt cartilage differentiation occurs (Smits et al., 2001). A conditional allele of mouse *Sox9* has been made (Kist et al., 2002), which should facilitate phenotypic analysis of skeletal development in homozygous *Sox9* mutant mice.

The simultaneous failure of chondrocyte differentiation and morphogenesis of condensations in *jef* (*sox9a*) mutants suggests that *jef* (*sox9a*) regulates both morphogenesis and differentiation, and provides another example of specification and morphogenesis going hand-in-hand (see Kimmel et al., 2001a; Kimmel et al., 2001b). These morphogenetic processes are separable from differentiation: the zebrafish *pipetail* [*ppt* (*wnt5a*)] mutation (Piotrowski et al., 1996; Rauch et al., 1997; Hammerschmidt et al., 1996) disrupts chondrocyte stacking but not differentiation. Thus, differentiation does not require stacking. Likewise, individuation of cartilage elements occurs in *ppt* (*wnt5a*) mutants (Piotrowski et al., 1996), suggesting that the *jef* (*sox9a*)-dependent morphogenetic processes are distinct aspects of morphogenesis under regulation of separate loci.

The failure of differentiation and morphogenesis in *jef* (*sox9a*) mutants correlates in time and space with the *col2a1* expression defect, and raises the possibility that *col2a1* might be involved in one or both of these processes. Because COL2A is a major component of differentiated cartilage matrix (Vandenberg et al., 1991), perhaps zebrafish *col2a1* is required for cartilage differentiation, and the failure to activate *col2a1* expression underlies the near complete absence of cartilage in *jef* (*sox9a*) mutants. The lack of Col2a might also underlie the morphogenetic defects in *jef* (*sox9a*) mutants – it is possible that cells require a normal extracellular matrix in order to exhibit stacking cell behaviors. It would be interesting to see if exogenously supplied Col2a could rescue either morphogenesis (e.g. stacking) or differentiation in *jef* (*sox9a*) mutants.

SOX9 regulates not only *COL2A1,* but other downstream targets as well. *SOX9* positively regulates expression of *CDH2* (Panda et al., 2001), which may mediate the *jef* (*sox9a*)-dependent stacking, individuation or shaping of pharyngeal mesenchymal cells. Comparing expression of cadherin genes, *col2a1* and orthologs of other *Sox9* downstream targets in *ppt* and *jef* mutants might suggest which genetic pathways underlie stacking behavior and which cartilage differentiation. *SOX9* also regulates cell cycle genes (Panda et al., 2001), providing another potential mechanism for the differentiation and morphogenetic defects in *jef* (*sox9a*) mutants. Mitotic activity is enriched at the second arch dorsal/ventral joint, and was proposed to partially drive the extension of the symplectic cartilage (Kimmel et al., 1998). This region of the second arch condensation never extends in *jef* (*sox9a*) mutants, possibly because mitotic behavior of cells within the precartilage condensation is defective.

Pharyngeal muscle and bone differentiates in the absence of differentiated cartilage

Cranial neural crest (CNC) patterns the pharyngeal musculature according to Noden's experiments transplanting presumptive first arch CNC into the position of presumptive second arch CNC (Noden, 1983). Although recently reinterpreted to be due to the organizing effects of a transplanted isthmus (Trainor et al., 2002), the conclusion remains that the transplant non-autonomously induced host second arch muscles to adopt patterns appropriate to the first arch muscles. Further evidence for an instructive role of CNC comes from the zebrafish mutant *chinless* (*chw*), which lacks both differentiated pharyngeal cartilage and muscles (Schilling et al., 1996). Wild-type CNC cells, when transplanted into homozygous *chw* mutant hosts, induced local differentiation of pharyngeal muscles (Schilling et al., 1996). A third study revealed severe ventral muscle defects in pharyngeal arches of *suc* (*edn1*) mutants, although mutant cells contributed to normal ventral muscles when transplanted into a wild-type host (Miller et al., 2000). These results support the idea that signaling from the CNC patterns the pharyngeal arch mesoderm. The populations of CNC which participate in this signaling, however, remain unidentified. The CNC-derived muscle connective tissue (Kontges and Lumsden, 1996) is a candidate for this activity. The widespread expression of *sox9a* raises the possibility that *jef* (*sox9a*) might function in a CNC-derived connective tissue lineage. The skeletogenic CNC derivatives, some of which are perturbed in *jef* (*sox9a*) mutants, could also signal to the pharyngeal musculature. The presence of a normal pattern of differentiated pharyngeal muscles in *jef* (*sox9a*) mutants shows that signals from CNC to the surrounding mesoderm occur independently of *jef* (*sox9a*) function. Muscles in *jef* (*sox9a*) mutants are shorter and thicker that their wild-type counterparts, suggesting that elongation of the muscles might require stiff, differentiated cartilage.

The precocious ossification and expanded ossification centers in heterozygous *Sox9* mutant mice motivated the characterization of bone formation in *jef* (*sox9a*) mutants. Our calcein labeling confirms observations of bone (Piotrowski et al., 1996), and further demonstrates that cranial and pectoral fin bones form relatively normally in *jef* (*sox9a*) mutants, with the exceptions of the dentary and fifth ceratobranchial bone, a cartilage replacement bone (see Cubbage and Mabee, 1996) that appears to be surrounded by perichondral bone in wild-type 5-day-old zebrafish larvae. The absence of the fifth ceratobranchial bone in *jef* (*sox9a*) mutants could be explained if perichondral ossification requires a cartilage template. The dentary bone, a dermal bone (see Cubbage and Mabee, 1996), is intimately associated with Meckel's cartilage in wild type. Perhaps the reduction of the dentary in *jef* (*sox9a*) mutants is also secondary to the cartilage defect. Weaker alleles of zebrafish *jef* (*sox9a*) might allow analysis of bone development past the early larval stage of currently available alleles.

Because dermal bones appear without a cartilage template, it might not seem surprising that most dermal bones form normally in *jef* (*sox9a*) mutants. The widespread expression of *sox9a* in postmigratory CNC, however, suggests that CNC osteocyte precursors might express *sox9a*. Expression of *sox9a*, like that of *dlx2* in the zebrafish pharyngeal arches, appears to include the entire CNC population within each arch. The *dlx2*-expressing postmigratory CNC forms a cylinder surrounding the central cores of paraxial mesoderm (Miller et al., 2000; Kimmel et al., 2001a). This population presumably includes precursors of both the cartilage and bone skeleton, based on existing fate maps (Couly and Le Douarin, 1988; Schilling and Kimmel, 1997; Kontges and Lumsden, 1996). Thus, the absence of a major bone defect suggests that *jef* (*sox9a*) function in the pharyngeal skeleton might actually be required only in a subset of *sox9a*-expressing postmigratory CNC cells, the chondrocyte lineage. Fate-mapping experiments will determine whether chondrocytes and osteocytes share a lineage in the CNC, and whether the chondrocyte lineage is uniquely perturbed in *jef* (*sox9a*) mutants.

Sox9 and gene duplication

Xenopus embryos treated with a morpholino antisense oligonucleotide that inhibits the production of Sox9 protein lack neural crest progenitors, suggesting that Sox9 is essential for the specification of neural crest in frogs (Spokony et al., 2002). By contrast, neural crest specification is apparently normal in individuals with CD, because they make cranial crest derivatives, but just have hypoplastic skeletons, and in the absence of *sox9a* function in zebrafish, because the expression of *dlx2* is normal, the cranial crest migrates on schedule, and precartilage condensations form. How can we understand these differences? We hypothesize that *SOX9* may play multiple essential roles in cranial crest development, and that these may be revealed by further analysis of the two *SOX9* duplicates in zebrafish. As demonstrated by the work on *Xenopus* (Spokony

et al., 2002), Sox9 protein plays an early role in crest specification, and as revealed by our experiments on zebrafish and work with mouse, *sox9* plays a later role in chondrocyte differentiation that includes the regulation of *col2a1* and the morphogenesis that accomplishes stacking. Because the antisense methodology blocked the early step of crest specification in *Xenopus*, it was not possible to determine whether *Sox9* is required for the later morphogenetic roles. Zebrafish has two orthologs of *SOX9* that have diverged in sequence and expression pattern. The *sox9b* gene is expressed early in the neural crest of the head and body axis, like the *Xenopus Sox9* gene (Chiang et al., 2001; Li, 2002). We predict that *sox9b* may be necessary for the neural crest specification function revealed in *Xenopus* (Spokony et al., 2002), and that *sox9a* is necessary for the later step, as revealed by the *jef* (*sox9a*) mutations studied here. In the haploinsufficient mammalian mutants, the level of *SOX9* activity is likely to be half the normal level, and this may be sufficient for the early role in neural crest specification, and for much, but not all of the later role in cartilage morphogenesis.

The genome duplication that occurred in the ancestry of zebrafish (Amores et al., 1998; Postlethwait et al., 1998) was followed by nonfunctionalization so that zebrafish retains duplicate orthologs of about 30% of tetrapod genes (Postlethwait et al., 2000). Because subfunctionalization may preserve duplicate genes (Force et al., 1999; Stoltzfus, 1999), ancestral functions may assort to different duplicate copies. The expression patterns of *sox9a* and *sox9b* (Chiang et al., 2001) show overlapping subsets of the tetrapod *SOX9* expression pattern (Spokony et al., 2002; Wright et al., 1995), consistent with the hypothesis of subfunctionalization. Such subfunctionalization can reveal gene functions that are hidden by analysis of morpholino-injected animals or knock-out mutations in tetrapods because the absence of an early function in a cell lineage may preclude the detection of later functions. As has been the case with Nodal genes, where analysis of zebrafish co-orthologs of *Nodal* revealed an early function in the induction of mesoderm, and a previously obscured later function in neural plate patterning (Feldman et al., 1998; Sampath et al., 1998; Rebagliati et al., 1998; Blader and Strahle, 1998; Nomura and Li, 1998). Such may be the case with *sox9a* and *sox9b* as well. In particular, the early expression of *sox9b* in cranial crest may provide protein that might persist and partially compensate for the loss of *sox9a* function, even though *sox9b* is not expressed in post-migratory crest. Further analysis of *sox9b* can test these possibilities.

Supported by NIH grants R01RR10715 (J. H. P.), R01 DC04186 (M. W.), R01DE13834 (C. K.), RO1 RR12589 (N. H.), and P01HD22486 (C. K., J. H. P., M. W.); NSF grant IBN-9728587 (J. H. P), and a grant from Amgen (N. H.). We thank the NIH (1-G20-RR11724), NSF (STI-9602828), M. J. Murdock Charitable Trust (96127:JVZ:02/27/97) and W. M. Keck Foundation (961582) for supporting renovation of the University of Oregon Zebrafish Facility.

REFERENCES

Akimenko, M.-A., Ekker, M., Wegner, J., Lin, W. and Westerfield, M. (1994). Combinatorial expression of three zebrafish genes related to *Distal-less*: part of a homeobox gene code for the head. *J. Neurosci.* **14**, 3475-3486.

Amores, A., Force, A., Yan, Y.-L., Joly, L., Amemiya, C., Fritz, A., Ho, R. K., Langeland, J., Prince, V., Wang, Y.-L. et al. (1998). Zebrafish *hox* clusters and vertebrate genome evolution. *Science* **282**, 1711-1714.

Amsterdam, A., Burgess, S., Golling, G., Chen, W. B., Sun, Z. X., Townsend, K., Farrington, S., Haldi, M. and Hopkins, N. (1999). A large-scale insertional mutagenesis screen in zebrafish. *Genes Dev.* **13**, 2713-2724.

Bell, D. M., Leung, K. K., Wheatley, S. C., Ng, L.-J., Zhou, S., Ling, K. W., Sham, M. H., Koopman, P., Tam, P. P. L. and Cheah, K. S. E. (1997). SOX9 directly regulates the type-II collagen gene. *Nat. Genet.* **16**, 174-178.

Bi, W., Deng, J. M., Zhang, Z., Behringer, R. R. and de Crombrugghe, B. (1999). *Sox9* is required for cartilage formation. *Nat. Genet.* **22**, 85-89.

Bi, W., Huang, W., Whitworth, D. J., Deng, J. M., Zhang, Z., Behringer, R. R. and de Crombrugghe, B. (2001). Haploinsufficiency of *Sox9* results in defective cartilage primordia and premature skeletal mineralization. *Proc. Natl. Acad. Sci. USA* **98**, 6698-6703.

Blader, P. and Strähle, U. (1998). Developmental biology: casting an eye over cyclopia. *Nature* **395**, 112-113.

Burgess, S. and Hopkins, N. (2000). Use of pseudotyped retroviruses in zebrafish as genetic tags. *Methods Enzymol.* **327**, 145-161.

Cameron, F. J., Hageman, R. M., Cooke-Yarborough, C., Kwok, C., Goodwin, L. L., Sillence, D. O. and Sinclair, A. H. (1996). A novel germ line mutation in SOX9 causes familial campomelic dysplasia and sex reversal. *Hum. Mol. Genet.* **5**, 1625-1630.

Cancedda, R., Descalzi Cancedda, F. and Castagnola, P. (1995). Chondrocyte differentiation. *Int. Rev. Cytol.* **159**, 265-358.

Chiang, E., Pai, C.-I., Wyatt, M., Yan, Y.-L., Postlethwait, J. and Chung, B.-C. (2001). Two *sox9* genes on duplicated zebrafish chromosomes: expression of similar transcription activators in distinct sites. *Dev. Biol.* **229**, 149-163.

Childs, S., Weinstein, B. M., Mohideen, M. A. P. K., Donohue, S., Bonkovsky, H. and Fishman, M. C. (2000). Zebrafish *dracula* encodes ferrochelatase and its mutation provides a model for erythropoietic protoporphyria. *Curr. Biol.* **10**, 1001-1004.

Connor, F., Cary, P. D., Read, C. M., Preston, N. S., Driscoll, P. C., Denny, P., Crane-Robinson, C. and Ashworth, A. (1994). DNA binding and bending properties of the post-meiotically expressed Sry-related protein Sox-5. *Nucleic Acids Res.* **22**, 3339-3346.

Cooper, M. S., D'Amico, L. A. and Henry, C. A. (1999). Analyzing morphogenetic cell behaviors in vitally stained zebrafish embryos. *Methods Mol. Biol.* **122**, 185-204.

Cooper, M. S. and Kimmel, C. B. (1998). Morphogenetic cell behaviors during early teleost development. In *Motion Analysis in Living Cells* (ed. D. R. Soll), pp. 198-219. New York: Wiley-Liss.

Couly, G. and le Douarin, N. M. (1988). The fate map of the cephalic neural primordium at the presomitic to the 3-Somite stage in the avian embryo. *Development* **103**, 101-113.

Crow, J. F. (1950). *Genetic Notes*. Minneapolis: Burgess Publishing.

Cubbage, C. C. and Mabee, P. M. (1996). Development of the cranium and paired fins in the zebrafish, *Danio rerio* (Ostariophysi, cyprinidae). *J. Morphol.* **229**, 121-160.

de Crombrugghe, B., Lefebvre, V. and Nakashima, K. (2001). Regulatory mechanisms in the pathways of cartilage and bone formation. *Curr. Opin. Cell Biol.* **13**, 721-727.

Draper, B. W., Morcos, P. A. and Kimmel, C. B. (2001). Inhibition of zebrafish *fgf8* pre-mRNA splicing with morpholino oligos: A quantifiable method for gene knockdown. *Genesis* **30**, 154-156.

Du, S.J., Frenkel, V., Kindschi, G. and Zohar, Y. (2001). Visualizing normal and defective bone development in zebrafish embryos using the fluorescent chromophore calcein. *Dev. Biol.* **238**, 239-246.

Feldman, B., Gates, M., Egan, E. S., Dougan, S. T., Rennebeck, G., Sirotkin, H. I., Schier, A. F. and Talbot, W. S. (1998). Zebrafish organizer development and germ-layer formation require nodal-related signals. *Nature* **395**, 181-185.

Force, A., Lynch, M., Pickett, F. B., Amores, A., Yan, Y.-L. and Postlethwait, J. (1999). Preservation of duplicate genes by complementary, degenerative mutations. *Genetics* **151**, 1531-1545.

Foster, J. W., Dominguez-Steglich, M. A., Guioli, S., Kwock, C., Weller, P. A., Stevanovic, M., Weissenbach, J., Mansour, S., Young, I. D., Goodfellow, P. N. et al. (1994). Campomelic dysplasia and autosomal sex reversal caused by mutations in an *SRY*-related gene. *Nature* **372**, 525-530.

Freddi, S., Savarirayan, R. and Bateman, J. F. (2000). Molecular diagnosis of Stickler syndrome: a COL2A1 stop codon mutation screening strategy

that is not compromised by mutant mRNA instability. *Am. J. Med. Genet.* **90**, 398-406.

Fritz, A., Rozowski, M., Walker, C. and Westerfield, M. (1996). Identification of selected gamma-ray induced deficiencies in zebrafish using multiplex polymerase chain reaction. *Genetics* **144**, 1735-1745.

Grandel, H. and Schulte-Merker, S. (1998). The development of the paired fins in the zebrafish (*Danio rerio)*. *Mech. Dev.* **79**, 99-120.

Hageman, R. M., Cameron, F. J. and Sinclair, A. H. (1998). Mutation analysis of the SOX9 gene in a patient with campomelic dysplasia. *Hum. Mutat.* **1**, S112-S113.

Hamerman, D. (1989). The biology of osteoarthritis. *New Engl. J. Med.* **320**, 1322-1330.

Hammerschmidt, M., Pelegri, F., Mullins, M. C., Kane, D. A., Brand, M., van Eeden, F. J., Furutani-Seiki, M., Granato, M., Haffter, P., Heisenberg, C.-P. et al. (1996). Mutations affecting morphogenesis during gastrulation and tail formation in the zebrafish, *Danio rerio*. *Development* **123**, 143-151.

Houston, C. S., Opitz, J. M., Spranger, J. W., Macpherson, R. I., Reed, M. H., Gilbert, E. F., Herrmann, J. and Schinzel, A. (1983). The campomelic syndrome: review, report of 17 cases, and follow-up on the currently 17-year-old boy first reported by Maroteaux et al., in 1971. *Am. J. Med. Genet.* **15**, 3-28.

Huang, B., Wang, S., Ning, Y., Lamb, A. N. and Bartley, J. (1999). Autosomal XX sex reversal caused by duplication of SOX9. *Am. J. Med. Genet.* **87**, 349-353.

Huang, W., Chung, U.-I., Kronenberg, H. M. and de Crombrugghe, B. (2001). The chondrogenic transcription factor *Sox9* is a target of signaling by the parathyroid hormone-related peptide in the growth plate of endochondral bones. *Proc. Natl. Acad. Sci. USA* **98**, 160-165.

Johnson, R. F., Pickett, S. C. and Barker, D. L. (1990). Autoradiography using storage phosphor technology. *Electrophoresis* **11**, 355-360.

Jowett, T. and Yan, Y. L. (1996). Double fluorescent in situ hybridization to zebrafish embryos. *Trends Genet.* **12**, 387-389.

Kimmel, C. B., Miller, C. T., Kruze, G., Ullmann, B., BreMiller, R. A., Larison, K. D. and Snyder, H. C. (1998). The shaping of pharyngeal cartilages during early development of the zebrafish. *Dev. Biol.* **203**, 246-263.

Kimmel, C. B., Miller, C. T. and Keynes, R. J. (2001a). Neural crest patterning and the evolution of the jaw. *J. Anat.* **199**, 105-120.

Kimmel, C. B., Miller, C. T. and Moens, C. B. (2001b). Specification and morphogenesis of the zebrafish larval head skeleton. *Dev. Biol.* **233**, 239-257.

Kist, R., Schrewe, H., Balling, R. and Scherer, G. (2002). Conditional inactivation of *Sox9*: A mouse model for campomelic dysplasia. *Genesis* **32**, 121-123.

Knapik, E., Goodman, A., Ekker, M., Chevrette, M., Delgado, J., Neuhauss, S., Shimoda, N., Driever, W., Fishman, M. and Jacob, H. (1998). A microsatellite genetic linkage map for zebrafish (*Danio rerio*). *Nat. Genet.* **18**, 338-343.

Kontges, G. and Lumsden, A. (1996). Rhombencephalic neural crest segmentation is preserved throughout craniofacial ontogeny. *Development* **122**, 3229-3242.

Kreivi, J.-P. and Lamond, A. I. (1996). RNA splicing: unexpected spliceosome diversity. *Curr. Biol.* **6**, 802-805.

Kwok, C., Weller, P. A., Guioli, S., Foster, J. W., Mansour, S., Zuffardi, O., Punnett, H. H., Domiguez-Steglich, M. A., Brook, J. D., Young, I. D. et al. (1995). Mutations in SOX9, the gene responsible for Campomelic dysplasia and autosomal sex reversal. *Am. J. Hum. Genet.* **57**, 1028-1036.

Labeit, S. and Kolmerer, B. (1995). Titins: giant proteins in charge of muscle ultrastructure and elasticity. *Science* **270**, 293-296.

Lefebvre, V., Huang, W., Harley, V. R., Goodfellow, P. N. and de Crombrugghe, B. (1997). SOX9 is a potent activator of the chondrocyte-specific enhancer of the pro alpha1(II) collagen gene. *Mol. Cell. Biol.* **17**, 2336-2346.

Li, M., Zhao, C., Wang, Y., Zhao, Z. and Meng, A. (2002) Zebrafish sox9b is an early neural crest marker. *Dev. Genes Evol.* **212**, 203-206.

Lun, K. and Brand, M. (1998). A series of *no isthmus* (*noi*) alleles of the zebrafish *pax2.1* gene reveals multiple signaling events in development of the midbrain-hindbrain boundary. *Development* **125**, 3049-3062.

Mansour, S., Hall, C. M., Pembrey, M. E. and Young, I. D. (1995). A clinical and genetic study of campomelic dysplasia. *J. Med. Genet.* **32**, 415-420.

McKusick, V. A. (1990). Campomelic dwarfism. MIM no. 211970. In *Mendelian Inheritance in Man.* Baltimore, MD: Johns Hopkins University Press.

Miller, C. T., Schilling, T. F., Lee, K., Parker, J. and Kimmel, C. B. (2000). *sucker* encodes a zebrafish Endothelin-1 required for ventral pharyngeal arch development. *Development* **127**, 3815-3828.

Moens, C. B., Yan, Y.-L., Appel, B., Force, A. G. and Kimmel, C. B. (1996). *valentino*: a zebrafish gene required for normal hindbrain segmentation. *Development* **122**, 3981-3990.

Morais da Silva, S., Hacker, A., Harley, V., Goodfellow, P. N., Swain, A. and Lovell-Badge, R. (1996). *Sox9* expression during gonadal development implies a conserved role for the gene in testis differentiation in mammals and birds. *Nat. Genet.* **14**, 62-68.

Mount, S. (1982). A catalogue of splice junction sequences. *Nucleic Acids Res.* **10**, 459-472.

Müller, H. J. (1932). Further studies on the nature and causes of gene mutations. *Int. Congr. Genet.* **6**, 213-255.

Ng, L.-J., Wheatley, S., Muscat, G. E. O., Conway-Campbell, J., Bowles, J., Wright, E., Bell, D. M., Tam, P. P. L., Cheah, K. S. E. and Koopman, P. (1997). SOX9 binds DNA, activates transcription, and coexpresses with type II collagen during chondrogenesis in the mouse. *Dev. Biol.* **183**, 108-121.

Noden, D. M. (1983). The role of the neural crest in patterning of avian cranial skeletal, connective, and muscle tissues. *Dev. Biol.* **96**, 144-165.

Nomura, M. and Li, E. (1998). *Smad2* role in mesoderm formation, left-right patterning and craniofacial development. *Nature* **393**, 786-790.

Ohe, K., Lalli, E. and Sassone-Corsi, P. (2002). A direct role of SRY and SOX proteins in pre-mRNA splicing. *Proc. Natl. Acad. Sci. USA* **99**, 1146-1151.

Panda, D. K., Miao, D., Lefebvre, V., Hendy, G. N. and Goltzman, D. (2001). The transcription factor SOX9 regulates cell cycle and differentiation genes in chondrocytic CFK2 cells. *J. Biol. Chem.* **276**, 41229-41236.

Piotrowski, T., Schilling, T. F., Brand, M., Jiang, Y. J., Heisenberg, C.-P., Beuchle, D., Grandel, H., van Eeden, F. J., Furutani-Seiki, M., Granato, M. et al. (1996). Jaw and branchial arch mutants in zebrafish II: anterior arches and cartilage differentiation. *Development* **123**, 345-356.

Postlethwait, J., Johnson, S., Midson, C. N., Talbot, W. S., Gates, M., Ballenger, E. W., Africa, D., Andrews, R., Carl, T., Eisen, J. S. et al. (1994). A genetic linkage map for the zebrafish. *Science* **264**, 699-703.

Postlethwait, J. H., Yan, Y.-L., Gates, M., Horne, S., Amores, A., Brownlie, A., Donovan, A., Egan, E., Force, A., Gong, Z. et al. (1998). Vertebrate genome evolution and the zebrafish gene map. *Nat. Genet.* **18**, 345-349.

Postlethwait, J. H., Woods, I. G., Ngo-Hazelett, P., Yan, Y.-L., Kelly, P. D., Chu, F., Huang, H., Hill-Force, A. and Talbot, W. S. (2000). Zebrafish comparative genomics and the origins of vertebrate chromosomes. *Genome Res.* **10**, 1890-1902.

Rauch, G.-J., Hammerschmidt, M., Blader, P., Schauerte, H. E., Strähle, U., Ingham, P. W., McMahon, A. P. and Haffter, P. (1997). WNT5 is required for tail formation in the zebrafish embryo. *Cold Spring Harb. Symp. Quant. Biol.* **62**, 227-233.

Rebagliati, M. R., Toyama, R., Haffter, P. and Dawid, I. B. (1998). *cyclops* encodes a nodal-related factor involved in midline signaling. *Proc. Natl. Acad. Sci. USA* **95**, 9932-9937.

Sampath, K., Rubinstein, A. L., Cheng, A. M., Liang, J. O., Fekany, K., Solnica-Krezel, L., Korzh, V., Halpern, M. E. and Wright, C. V. (1998). Induction of the zebrafish ventral brain and floorplate requires *cyclops*/nodal signalling. *Nature* **395**, 185-189.

Schilling, T. F. and Kimmel, C. B. (1997). Musculoskeletal patterning in the pharyngeal segments of the zebrafish embryo. *Development* **124**, 2945-2960.

Schilling, T. F., Walker, C. and Kimmel, C. B. (1996). The *chinless* mutation and neural crest interactions in zebrafish jaw development. *Development* **122**, 1417-1426.

Shimoda, N., Knapik, E. W., Ziniti, J., Sim, C., Yamada, E., Kaplan, S., Jackson, D., de Sauvage, F., Jacob, H. and Fishman, M. C. (1999). Zebrafish genetic map with 2000 microsatellite markers. *Genomics* **58**, 219-232.

Schmajuk, G., Sierakowska, H. and Kole, R. (1999). Antisense oligonucleotides with different backbones: modification of the splicing pathway and efficacy of uptake. *J. Biol. Chem.* **274**, 21783-21789.

Smits, P., Li, P., Mandel, J., Zhang, Z., Deng, J. M., Behringer, R. R., de Crombrugghe, B. and Lefebvre, V. (2001). The transcription factors L-Sox5 and Sox6 are essential for cartilage formation. *Dev. Cell* **1**, 277-290.

Sironi, M., Corti, S., Locatelli, F., Cagliani, R. and Comi, G. P. (2001). A novel splice site mutation (3157+1G>T) in the dystrophin gene causing total exon skipping and DMD phenotype. *Hum. Mutat.* **17**, 239.

Spokony, R., Aoki, Y., Saint-Germain, N., Magner-Fink, E. and Saint-Jeannet, J. (2002). The transcription factor *Sox9* is required for cranial neural crest development in *Xenopus*. *Development* **129**, 421-432.

Stoltzfus, A. (1999). On the possibility of constructive neutral evolution. *J. Mol. Evol.* **49**, 169-181.

Südbeck, P., Schmitz, M. L., Baeuerle, P. A. and Scherer, G. (1996). Sex reversal by loss of the C-terminal transactivation domain of human SOX9. *Nat. Genet.* **13**, 230-232.

Targovnik, H. M., Rivolta, C. M., Mendive, F. M., Moya, C. M., Vono, J. and Medeiros-Neto, G. (2001). Congenital goiter with hypothyroidism caused by a 5′ splice site mutation in the thyroglobulin gene. *Thyroid* **11**, 685-690.

Trainor, P. A., Ariza-McNaughton, L. and Krumlauf, R. (2002). Role of the *isthmus* and FGFs in resolving the paradox of neural crest plasticity and prepatterning. *Science* **295**, 1288-1291.

Vandenberg, P., Khillan, J. S., Prockop, D. J., Helminen, H., Kontusaari, S. and Ala-Kokko, L. (1991). Expression of a partially deleted gene of human type II procollagen (COL2A1) in transgenic mice produces a chondrodysplasia. *Proc. Natl. Acad. Sci. USA* **88**, 7640-7644.

van Eeden, F. J. M., Granato, M., Schach, U., Brand, M., Furutani-Seiki, M., Haffter, P., Hammerschmidt, M., Heisenberg, C. P., Jiang, Y. J., Kane, D. A. et al. (1996). Genetic analysis of fin formation in the zebrafish, *Danio rerio*. *Development* **123**, 255-262.

Vidal, V. P. I., Chaboissier, M. C., de Rooij, D. G. and Schedl, A. (2001). *Sox9* induces testis development in XX transgenic mice. *Nat. Genet.* **28**, 216-217.

Wagner, T., Wirth, J., Meyer, J., Zabel, B., Held, M., Zimmer, J., Pasantes, J., Bricarelli, F. D., Keutel, J. and Hustert, E. (1994). Autosomal sex reversal and campomelic dysplasia are caused by mutations in and around the *SRY*-related gene *SOX9*. *Cell* **79**, 111-1120.

Wegner, M. (1999). From head to toes: the multiple facets of Sox proteins. *Nucleic Acids Res.* **27**, 1409-1420.

Werner, M. H., Huth, J. R., Gronenborn, A. M. and Clore, G. M. (1995). Molecular basis of human 46X,Y sex reversal revealed from the three-dimensional solution structure of the human SRY-DNA complex. *Cell* **81**, 705-714.

Westerfield, M. (2001). *The Zebrafish Book: A Guide for the Laboratory Use of Zebrafish (*Danio rerio*).* Eugene: University of Oregon Press.

Woods, I. G., Kelly, P. D., Chu, F., Ngo-Hazelett, P., Yan, Y.-L., Huang, H., Postlethwait, J. H. and Talbot, W. S. (2000). A comparative map of the zebrafish genome. *Genome Res.* **10**, 1903-1914.

Wright, E., Hargrave, M. R., Christiansen, J., Cooper, L., Kun, J., Evans, T., Gangadharan, U., Greenfield, A. and Koopman, P. (1995). The *SRY*-related gene *Sox9* is expressed during chondrogenesis in mouse embryos. *Nat. Genet.* **9**, 15-20.

Wright, E. M., Snopek, B. and Koopman, P. (1993). Seven new members of the *Sox* gene family expressed during mouse development. *Nucleic Acids Res.* **21**, 744.

Wunderle, V. M., Critcher, R., Hastie, N., Goodfellow, P. N. and Schedl, A. (1998). Deletion of long-range regulatory elements upstream of SOX9 causes campomelic dysplasia. *Proc. Natl. Acad. Sci. USA* **95**, 10649-10654.

Xu, X., Meiler, S. E., Zhong, T. P., Mohideen, M. A., Crossley, D. A., Burggren, W. W. and Fishman, M. C. (2002). Cardiomyopathy in zebrafish due to mutation in an alternatively spliced exon of *titin*. *Nat. Genet.* **30**, 205-209.

Yan, Y.-L., Hatta, K., Riggleman, B. and Postlethwait, J. H. (1995). Expression of a type II collagen gene in the zebrafish embryonic axis. *Dev. Dyn.* **203**, 363-376.

Zhang, M. Q. (1998). Statistical features of human exons and their flanking regions. *Hum. Mol. Genet.* **7**, 919-932.

Zhao, Q., Eberspaecher, H., Lefebvre, V. and de Crombrugghe, B. (1997). Parallel expression of *Sox9* and *Col2a1* in cells undergoing chondrogenesis. *Dev. Dyn.* **209**, 377-386.